

Spin-splitting in 2D electron gas with Rashba spin orbit interaction as $B \rightarrow 0$



Sadia Rafi
Regn.#00000173014

A thesis submitted in partial fulfilment of the requirements
for the degree of **Master of Science**
in
Physics

Supervised by: Dr Rizwan Khalid

Department of Physics

School of Natural Sciences
National University of Sciences and Technology
H-12, Islamabad, Pakistan
The Year 2020

FORM TH-4

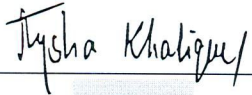
National University of Sciences & Technology

MS THESIS WORK

We hereby recommend that the dissertation prepared under our supervision by: Ms.Sadia Rafi, Regn No. 00000173014 Titled: "Spin-Splitting in 2D Electron Gas with Rashba Spin Orbit Interaction as $B \rightarrow 0$ " be accepted in partial fulfillment of the requirements for the award of **MS** degree.

Examination Committee Members

1. Name: Dr. Aeysha Khalique

Signature: 

2. Name: Dr. Muhammad Ali Paracha

Signature: 

External Examiner: Dr. Ghulam Hassnain

Signature: 

Supervisor's Name: Dr. Rizwan Khalid

Signature: 



Head of Department

30/9/2020
Date

COUNTERSIGNED

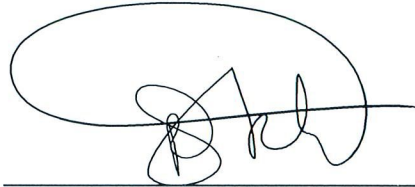
Date: 5/10/2020



Dean/Principal

THESIS ACCEPTANCE CERTIFICATE

Certified that final copy of MS thesis written by Ms.Sadia Rafi, (Registration No. 00000173014), of School of Natural Sciences has been vetted by undersigned, found complete in all respects as per NUST statutes/regulations, is free of plagiarism, errors, and mistakes and is accepted as partial fulfillment for award of MS/M.Phil degree. It is further certified that necessary amendments as pointed out by GEC members and external examiner of the scholar have also been incorporated in the said thesis.




Signature: _____

Name of Supervisor: Dr. Rizwan Khalid

Date: 30/9/2020

Signature (HoD): 

Date: 30/9/2020

Signature (Dean/Principal): 

Date: 5/10/2020

Abstract

A 2DEG is considered with the RSOI with external perpendicular magnetic field. We use green functions method to derive analytical expressions of the DOS of a 2DEG with RSOI. Further with the help of DOS we obtain analytical expressions of magnetoconductivities for up and down spin electrons. These conductivities oscillate with dissimilar frequencies and thus give us beating patterns of amplitude of SdH oscillations. If we know the magnetic field for any beat node through experiment, we can find a simplest equation that enables us to determine the ZFSS energy. The analytical results obtained in this research will reproduce the measured ZFSS energy, the amount of oscillations between two successive nodes and the non periodic beating patterns obtained through experiments

Contents

Abstract	1
List of Figures	4
List of Tables	6
List of Abbreviations	7
1 Introduction and motivation	1
2 Theory and Background	5
2.1 Two-dimensional electron system	5
2.1.1 Semiconductor Heterojunction	6
2.2 Semiconductor spintronics	9
2.2.1 Spin orbit interaction(SOI) in semiconductor con duction band	9
2.2.2 Dresselhaus spin orbit interaction	12
2.2.3 Rashba spin orbit interaction	13
2.3 Magnetotransport in 2DEG	16
2.3.1 The Drude Model and the Hall effect	16
2.3.2 The Integer Quantum Hall Effect (QHE)	19

2.3.3	Shubnikov-de Haas Oscillations	23
2.4	Single Particle Picture of 2DEG	26
2.4.1	Landau Quantization	26
2.4.2	Kinetic term	27
3	Methodology	32
3.0.1	Derivation of Hamiltonian	33
3.0.2	Eigenstates and Eigenvalues	38
3.0.3	Density of States	45
4	Results and Discussion	47
4.1	Analytic Results	47
4.2	Side by side assessment with known experiment	52
5	Conclusion	55
	Bibliography	56

List of Figures

2.1	(a)Schematic view of two dimensional electron system(b) Schematic view of semiconductor heterojunction. AlGaAs has higher Fermi energy and electron spills into GaAs, leaving positively charge donors behind. This cause a band bending and produces high electron density near the interface, the 2D electron gas.[25]	6
2.2	Figure showing three layer heterostructure with different energy gaps. Quantum well is created, if $E_{g,I}$ is small compared to other two layers, confining, in the z -direction, the charge density of the conduction band.[28]	8
2.3	Schematic view of production of effective magnetic field by RSOI “follows” the path of the electron.[27]	14
2.4	Schematic sketches of spin orientation due to Rashba and Dresselhaus effects. Here k_x is choosen to be [010], ky the [100] crystal diection and z is along [001]	15

2.5	(a) Measurement setup for the Hall effect with a sample of width W and length L . The Hall voltage V_{XY} can be measured between probes 3 and 5 or 4 and 6. (b) Plan view of (a) with the voltage probes removed and the current path of the charge carriers with the effects of magnetic field.[40]	18
2.6	From [43]. The voltage drop UPP and the Hall voltage UH between the probes (where UPP is equivalent to V_{xx} in figure 2-10) are both plotted as a function of the gate voltage V_g . Troughs and plateaus, signatures of the QHE, can be clearly seen in UPP and UH respectively.	20
2.7	: (a) At zero magnetic field ($B = 0$ T) the 2D DOS remains constant with increasing energy. With the increase in magnetic field, available states form group into Landau levels that are separated by the cyclotron energy as shown in (b) and (c).[40]	22
2.8	: (a) Fan diagram of first four E_n Plots (b) replacing vertical axis of energy with the sheet density.[40]	23
2.9	: Hall effect and SdH oscillations in a modulation-doped heterojunction of $GaAs/Ga_{0.7}Al_{0.3}As$ measured at 1.18 K. Electron density measured as $5.6 \times 10^{15} m^{-2}$ and mobility $15.3 m^2 (Vs)^{-1}$ [45].	25
3.1	Subband Energy E_s versus index s . The circles for $-$ branch and triangles for $+$ branch.	44
4.1	Plots of the analytical (solid) and exact (dashed) expressions of the total conductivities vs $1/B$	50
4.2	Plot of resistivity vs magnetic field B	52

List of Tables

4.1	Sample A:ZFSS and Rashba interaction SOI power at different node locations	53
4.2	Sample B: ZFSS and Rashba α SOI power at different node locations	54

List of Abbreviations

2D	Two Dimensions
2DEG	Two Dimensional Electron Gas
2DHG	Two Dimensional Hole Gas
BIA	Bulk Inversion Asymmetries
DOF	Degree of Freedom
DOS	Density of states
FET	Field Effect Transistor
RSOI	Rashba Spin Orbit Interaction
SdH	Shubnikov de Haas
SIA	Surface Inversion Asymmetries
SOC	Spin Orbit Coupling
SOI	Spin Orbit Interaction
ZFSS	Zero Field Spin Splitting

Chapter 1

Introduction and motivation

The spin orbit interaction pulls in a great deal of interest on account of its significance in basic principles of science and its practical applications. The SOI stems from special relativity. A recent investigation in semiconductor based devices has consolidated the spin degree of freedom as another state variable in novel electronic devices with potential for future applications. Due to spin freedom semiconductors provide over their insulating and metallic counterparts, i.e a small band-gap, that can be tuned by doping or applying an electric field in the form of a gate bias. This has lead to the advancement of bipolar and metaloxide-semiconductor transistors, utilized all through present day electronics. Moreover, as strategies for manufacturing semiconductor heterostructures have improved, so has the scope of semiconductor structures accessible for study. In low dimensional condensed matter systems, a lot of research and thought has been done with reference to the spin orbit interaction (SOI) for low dimensional condensed matter systems due to its potential uses in spin based electronic devices [1–3]. The SOI is responsible for the following major effects

- Spin-FET [4, 5]
- Metal insulator transition in a 2DHG[6]
- Spin-resolved ballistic transport [7]
- Spin-galvanic effect [8]
- Spin-Hall effect [8, 9]

A key motivating factor has been to measure and maintain the strength of SOI experimentally as it affects the spin degree of freedom.

Without external magnetic field, the SOI lets the two-fold spin degeneracy be lifted at the finite momenta of the electron. Furthermore, there are two key mechanisms responsible for the ZFSS in semiconductor hetero-structures, which are -the Dresselhaus interaction[11] which varies with k^3 followed by the Rashba interaction [12] varying linearly with k where k is the wave vector. The former is because of crystals' inversion asymmetry and the latter is due to asymmetric quantum wells. Asymmetric quantum wells generate electric field that results in the RSOI. It is also possible to tune an SOI with a very strong electric field externally which is at right angle to the planer of motion of the electrons. The Dresselhaus interaction is known for controlling wide-gap semiconductors with small thicknesses in contrast to Rashba interaction which controls narrow-gap semiconductors for they have different momentum dependencies [13, 14].

An immediate indication of the spin split levels is a beating change in the SdH oscillations because of the two firmly dispersed dissimilar frequencies of the spin down and up electrons. It was indicated that the RSOI produces customary beating patterns in SdH motions [14]. However, only odd beating patterns observed in

Dresselhaus interaction. The quality of an SOI can be observed by breaking down and analyzing the SdH oscillations.

An experimental evidence of ZFSS is observed in modulation doped GaAs/AlGaAs heterojunction [15, 16]. This evidence was found by utilizing the magnetotransport and cyclotron reverberation. At first, it was clarified by Bychkov and Rashba relying on the SOI created in the asymmetric quantum wells[17]. The ZFSS is identified with the Fermi wave vector k_F and the SOI's strength α as $\Delta_s = 2k_F\alpha$. The RSOI is viewed as the suitable effect for analyzing the ZFSS in low-dimensional quantum frameworks, especially in restricted narrow gap semiconductors. The beating oscillations in the SdH motions have been found in GaSb/InAs quantum wells and it has been confirmed that the rise of the spin decadence is because of the RSOI [18]. Afterward, Das et al.[19] examined the SdH oscillations in a progression of three different tweak doped heterostructures with high electron densities and confirmed that the lifting of the spin degeneracy is because of the RSOI. There are many proposed methods to control the strength of SOI in 2DEG of different materials [20–22].

It is notable that with magnetic field at low temperature and low magnetic fields SdH oscillations are produced. Extrapolating data along with model calculations for the SdH oscillations were used to find out the RSOI strength in ZFSS energy [23]. Moreover, the ZFSS theory was later studied based on contrast between self-consistent Born approximation and Landau energy levels [24]. The expected SOI strength was in a preferred pact with the generalized results acquired in [19].

In this dissertation, we focus on an approach to investigate the ZFSS energy in 2DEG. The systematic articulations of the SdH oscillations are also obtained. This result is for the up-down spin electrons. These oscillations are shown in the beating pattern of absolute magnetoconductivity because of two firmly separated

dissimilar frequencies of the SdH motions for up and down spin electrons. We follow up by investigating the beating patterns and discover a simple equation to decide the ZFSS energy from the area of any beat nodes. We likewise clarify systematically the number of fluctuations between the two consecutive nodes and the non-intermittent conduct of the beating patterns.

In chapter 2, there is a review of the basic concepts that are used throughout the thesis. This chapter mainly discusses the origin of SOI, magnetotransport properties and spin splitting in a 2DEG. It ends with the single particle picture of a 2DEG. Chapter 3 includes the derivation of Hamiltonian of our system by applying the non relativistic limit on the Dirac equation. In this chapter, we sum up the eigenvalues of energy and their related eigenfunctions of the system of 2DEG including RSOI and a right angled magnetic field. We also calculate the density of states by using imaginary part of self energy. Analytical and numerical results about SdH oscillations are discussed in chapter 4. In section 4.1, utilizing the accessible experimental data, we compute spin splitting energy when magnetic field approaches zero and number of fluctuations between two consecutive nodes from theoretical results. Experimental and theoretical results are compared in section 4.2. At the end, summary of the work is presented in chapter 5 along with recommendations for future work.

Chapter 2

Theory and Background

In this chapter, some basic definitions and concepts will be discussed briefly like two dimensional electron gas, SOI and its types, magneto-transport, integer quantum Hall effects and SdH oscillations. Some basic equations are derived like Hamiltonian and wave function of single particle moving in magnetic field etc.

2.1 Two-dimensional electron system

Many decades ago, the "2D electron gas" became the center of interest in semiconductor physics. Many publications and several groups are using this concept in their respective research fields because this 2D system not only provides basic research but also has many applications. An electron gas, which is free to move in 2D, but firmly restricted in third dimension. This causes quantized energy levels to move in third direction, which can be avoided for multiple problems. It seems the electrons to be 2D sheet ingrained in 3D world. Similarly, for holes it is called 2D hole gas. For example, as it can be seen in Fig. 2.1(a) that electrons are confined in a very

thin potential layer. A new quantum phenomenon will be observed if potential layer width is of the order of 10^{-9}m because the electrons' De-Broglie wavelength must be fitted in quantum well. This results into energy sub-bands i.e. (E_0, E_1, \dots) . The system will be called two dimensional system when energy separation of quantum levels of electrons i.e. $E_1 - E_0$ is greater than other energies like broadening (Γ) , thermal energy (kT) etc. Now in z-direction energy is fixed and electrons can move freely in xy-plane. Such systems have many interesting and useful applications.

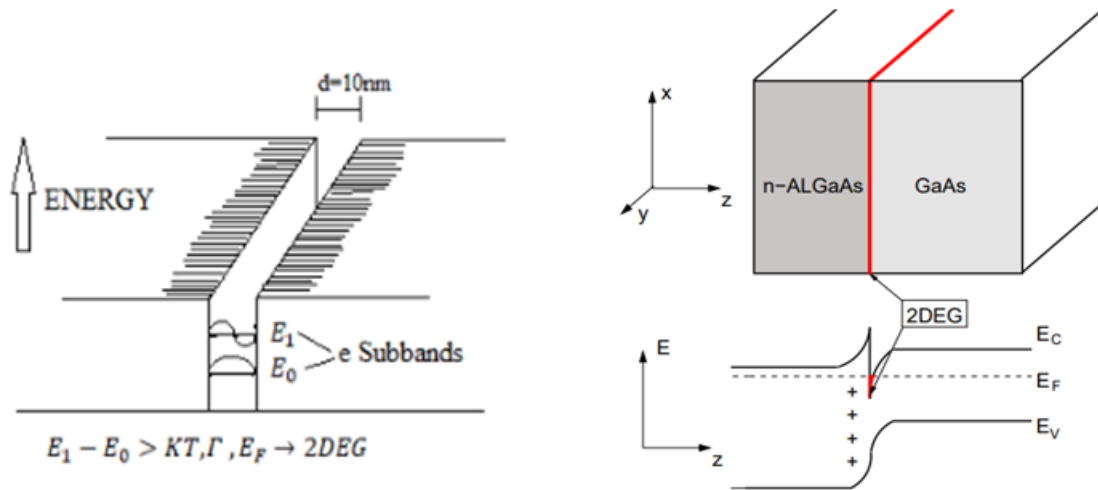


Figure 2.1: (a) Schematic view of two dimensional electron system (b) Schematic view of semiconductor heterojunction. AlGaAs has higher Fermi energy and electron spills into GaAs, leaving positively charged donors behind. This causes band bending and produces high electron density near the interface, the 2D electron gas. [25]

2.1.1 Semiconductor Heterojunction

Among the impactful scientific discoveries made in the early stages of 20th century physics was that non-artificial processes are impossible for actions lesser than $S =$

$\hbar/2$. The constraint is defined as the Heisenberg uncertainty principle. Processes occurring with action near the proximity of $\hbar/2$ it belongs to the quantum physics domain. Up till late stages of the twentieth century the unusual new existence was only seen, like within the atom. The changes due to advancement in physics allowed the manufacturing of artificial quantum systems. They are generally scaled in nanometers and at current time are Major interest in both fundamentals and applied research [26]. An adaptable platform for these man-made systems are semiconductor heterostructures (Fig. 2.1(b)), which are essentially, made of multi-layered distinct kinds of semi-conductors. Between the levels, jumps take place in the form of bands of energy We will be taking into consideration a case of two types of hetero-junction layers, under the assumption that, middle layers have less energy gaps compared to adjoining layers [27]. This will cause the formation of a quantum well towards the growth direction of the composition. Considering there is enough depth, only the last level in the direction of growth will be attainable to electrons within the band. This will cause effect in the electrons, withheld inside a place at right angles in the growth direction of 2DEG. This type of system can be seen in Fig. 2.2.

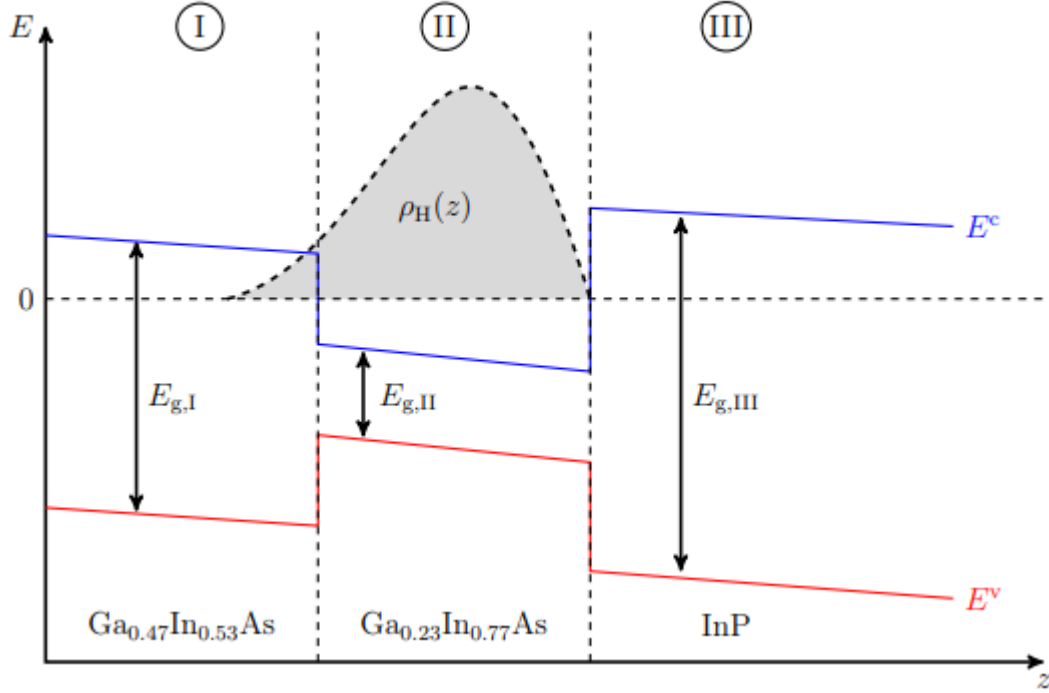


Figure 2.2: Figure showing three layer heterostructure with different energy gaps. Quantum well is created, if $E_{g,I}$ is small compared to other two layers, confining, in the z -direction, the charge density of the conduction band.[28]

In most pragmatic circumstances, where the vector \mathbf{k} is comparatively smaller than reciprocal of the lattice constant, it is to be expected that the electrons have a free energy scattering in 2DEG. Considering this supposition electron mass m_e is supplanted with m^* i.e effective mass. In k space, the relation between effective mass and the conduction band curvature can be shown as [29]

$$\frac{1}{m^*} = \frac{1}{\hbar^2} \frac{\partial^2 E_c}{\partial \mathbf{k}^2}$$

With the assistance of entryway cathodes, or by smart example manufacture, a huge

assortment of potential energy structures can be accomplished in the 2DEG.

2.2 Semiconductor spintronics

Normally charge in an electron is the key element, and warming the bench for the key element is the spin. Spintronics in electronics is when the spin will enact a vital role. Spintronics are the reason for the huge changes in metallic mediums of storing, due to success of finding GMR in 1988 [30]. Updating in semiconductor dominated spintronics allow more demanding and less paced. In spite of the fact that Supriyo Datta hypothetically proposed a turn FET in 1990 [31]. After couple of years it had yet to be recognized practically. A major challenge while producing these spintronics based gadgets was production of controlled field to generate rotations. After couple of years it had yet to be recognized practically. A major challenge while producing these spintronic based gadgets was production of controlled field to generate rotations. Effectively changing the field according to such sizes is not a practical. A solution to the identified issue is under study. The use of DMSC (dilute magnetic semiconductor) is a proposed solution [32]. Another is the manipulation of electrons using electricity based fields [33].

2.2.1 Spin orbit interaction (SOI) in semiconductor conduction band

As stated in the theory of special relativity, fields generated through electricity and magnets are Lorentz transformed when changes occur inside the inertial frame. hence for particles carrying charge and in motion inside a field, they begin to feel a field push on them within their inertial frame. A similar case due to this is

interactivity atoms i.e SOI. Powerful electronic fields of the particles combine with their spins, causing a Zeeman type separation of the spectral lines[34]. Is it possible that the aforementioned could allow the spin to be controlled conduction? Below is the emphasis of Hamiltonian H_{SO} , known as the Pauli spin-orbit term, displaying the spin-orbit interactivity:

$$H_{\text{SO}} = -\frac{\hbar}{4m_e^2c^2}\boldsymbol{\sigma} \cdot \mathbf{p} \times (\nabla V_0) \quad (2.1)$$

where

c = the speed of light

$\boldsymbol{\sigma} = (\sigma_x, \sigma_y, \sigma_z)$ = a vector of the Pauli matrices

V_0 = an electric potential

It can be derived from the non relativistic limit of Dirac equation[35]. Here, crystal potential will play the role of V_0 .

The electricity based field with most strength which an electron can experience is from the core of the atom. This allows outside effect to be considered null in the Pauli spin orbit term. The potential in crystals that is basically originated from core can be assumed radial near the core. According to this assumption we Pauli SO is termed as

$$H_{\text{SO}} \sim \mathbf{L} \cdot \mathbf{S}$$

Here

$\mathbf{L} = \mathbf{p} \times \mathbf{r}$ = orbital angular momentum operator

$\mathbf{S} = (\hbar/2)\boldsymbol{\sigma}$

Taking a start from excessively protected center through their valance electrons however more critically they are s like orbital electrons which implies that $\mathbf{L} =$

0. Better competitors, by a wide margin, would be the valence electrons. They experience bigger electric fields coming from nuclear centers and are p type orbital electrons, which implies that $\mathbf{L} = 1$. This is for sure the case for holes in the valence band which experience huge SOI[36].

The $\mathbf{k} \cdot \mathbf{p}$ method

The $\mathbf{k} \cdot \mathbf{p}$ approximation method is used for convenience to elaborate the SOI effects on energy band structure of the semiconductors. Bloch's theorem is used as a starting point in this method of approximation. For band n the wave function is

$$\Psi_{n,\mathbf{k}}(\mathbf{x}) = e^{i\mathbf{k}\cdot\mathbf{x}}u_{n,\mathbf{k}}(\mathbf{x})$$

where

$$u_{n,\mathbf{k}}(\mathbf{x}) = \text{Bloch function}$$

Both the Bloch's function and the crystal potential $V_0(\mathbf{x})$ has same periodicity. Using this information, Hamiltonian of the system including SOI can be written as [28]

$$H = \underbrace{\left[\frac{p^2}{2m_e} + V - \frac{\hbar}{4m_e^2c^2} \boldsymbol{\sigma} \cdot \mathbf{p} \times (\nabla V_0(\mathbf{x})) \right]}_{H_0} + \underbrace{\left[\frac{\hbar^2 k^2}{2m_e} + \frac{\hbar \mathbf{k} \cdot \boldsymbol{\pi}}{m_e} \right]}_{H'_k} \quad (2.2)$$

with

$$\boldsymbol{\pi} = \mathbf{p} + \frac{\hbar}{4m_e c^2} \boldsymbol{\sigma} \times (\nabla V_0(\mathbf{x}))$$

$|\mathbf{k}|$ is very small as compared to the reciprocal of lattice constant, so H'_k can be treated as perturbation. It is quite cumbersome task to find the spectrum of the above Hamiltonian. The standard beginning stage is to extend the Bloch function in

a premise of s and p like orbitals. In this premise the components of the Hamiltonian in Eq. (2.2) are

$$H_{n\sigma,n'\sigma'} = \left[E_{n'} + \frac{\hbar^2 k^2}{2m_e} \right] \delta_{n,n'} \delta_{\sigma,\sigma'} + \Delta_{n\sigma,n'\sigma'} + \frac{\hbar}{m_e} \mathbf{k} \cdot \mathbf{P}_{n\sigma,n'\sigma'} \quad (2.3)$$

and

$$\mathbf{P}_{n\sigma,n'\sigma'} = \langle n, \sigma | \boldsymbol{\pi} | n', \sigma' \rangle$$

shows inter band interaction and SO energy gap. With Eqs. (2.2) – (2.3) we have the way to investigate SO impacts in 2DEG. Two sorts of SO impacts are significant in 2DEG frameworks. These sorts are known as the Dresselhaus [11] and Rashba [12] SOI and emerge from a BIA and SIA, respectively

2.2.2 Dresselhaus spin orbit interaction

A system has time reversal balance without magnetic field. This satisfies the Kramer's theorem that is

$$E_{\uparrow}(\mathbf{k}) = E_{\downarrow}(-\mathbf{k})$$

If $H(\mathbf{x}) = -H(\mathbf{x})$, then both down and up spin energy levels are degenerate i.e.

$$E_{\uparrow}(\mathbf{k}) = E_{\downarrow}(\mathbf{k})$$

This avoids the impacts of SOC on the energy levels. Nonetheless, crystals with a zinc blende structure, for example GaAs, InAs, InP, etc., missing inversion symmetry. Because of this the spin degeneracy is expelled and we can expect impacts of SOC on the band structure. In mass structures the impacts of SOC on the

conduction band can be inferred to be [36, 37].

$$H_D \propto p_x[p_y^2 - p_z^2]\sigma_x + p_y[p_z^2 - p_x^2]\sigma_y + p_z[p_x^2 - p_y^2]\sigma_z \quad (2.4)$$

For 2 DEG structures developed in the [1,0,0] crystals heading Eq.(2.2) diminishes to

$$H_D = \frac{\beta}{\hbar}[\sigma_x k_x - \sigma_y k_y] \quad (2.5)$$

if we assume expectation value in the z direction and ignoring all terms that are in high order than \mathbf{p} . Where β is defined as the Dresselhaus term depending upon thickness of a 2DEG and the material band parameters.

2.2.3 Rashba spin orbit interaction

The Dresselhaus expression, Eq.(2.5), originates due to the crystal structure's inversion asymmetry and is completely dependent on material, aside from the thickness of a 2DEG. While, the Rashba SOI arises from an unnatural inversion asymmetry. Due to this reason it is easy to manipulate RSOI. As it is clear from the name, SOI generates interaction between its spin dynamics and the orbital motion of electron. If the electron travels through electric field, in its rest frame electric field is appeared to be moving. As a result, internal magnetic field is produced by moving charges in rest frame of electron which, in return, couples to electron spin. The direction and magnitude of internal magnetic field depends on velocity and traveling direction of electron in material i.e internal magnetic field is dependent on wave vector. When the electrons are restrained in asymmetrical potential to narrow layer 2D electron gas, their orbital and spin DOF (degree of freedoms) are coupled. This is known as rashba effect in which spin of electron having finite momentum experiences a mag-

netic field that is perpendicular to the momentum of electron in inversion symmetry. When magnetic field is absent, spin degeneracy of 2D electron gas energy bands is lifted by coupling of orbital motion of electron with its spin. This type of coupling arises due to asymmetric inversion of potential confined in 2DES. A natural clarification of the Rashba SOI is to see it in terms of an effective magnetic field. This can be done by changing the Rashba Hamiltonian with Zeeman like Hamiltonian

$$H_R = \frac{\alpha}{\hbar} \mathbf{z} \cdot (\boldsymbol{\sigma} \times \mathbf{p}) = \underbrace{\alpha(\mathbf{k} \times \mathbf{z})}_{\mathbf{B}_R(\mathbf{k})} \cdot \boldsymbol{\sigma}$$

This $\mathbf{B}_R(\mathbf{k})$ manifests itself as being always at right angle to the \mathbf{k} vector of the electron in the 2DEG, see Fig. 2.3

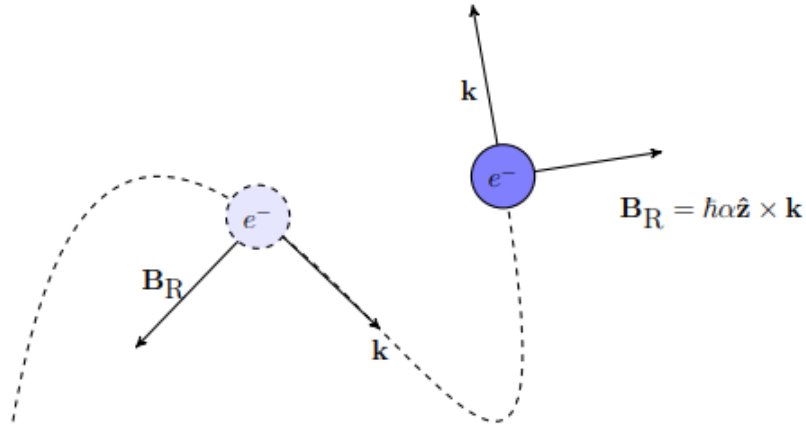


Figure 2.3: Schematic view of production of effective magnetic field by RSOI “follows” the path of the electron.[27]

The spin precession caused by RSOI occurs around the k_x direction along k_y direction and vice versa, as shown in Fig. 2.4(a), Fig. 2.4(b) and Fig. 2.4(c) show

the spin (precession axis) orientation for the linear and cubic term respectively. In an InGaAs 2DEG, the Rashba SOI is usually greater than Dresselhaus SOI. Thus in the thesis, we only focused on H_R by neglecting H_D to fit the low-field magnetoconductance data.

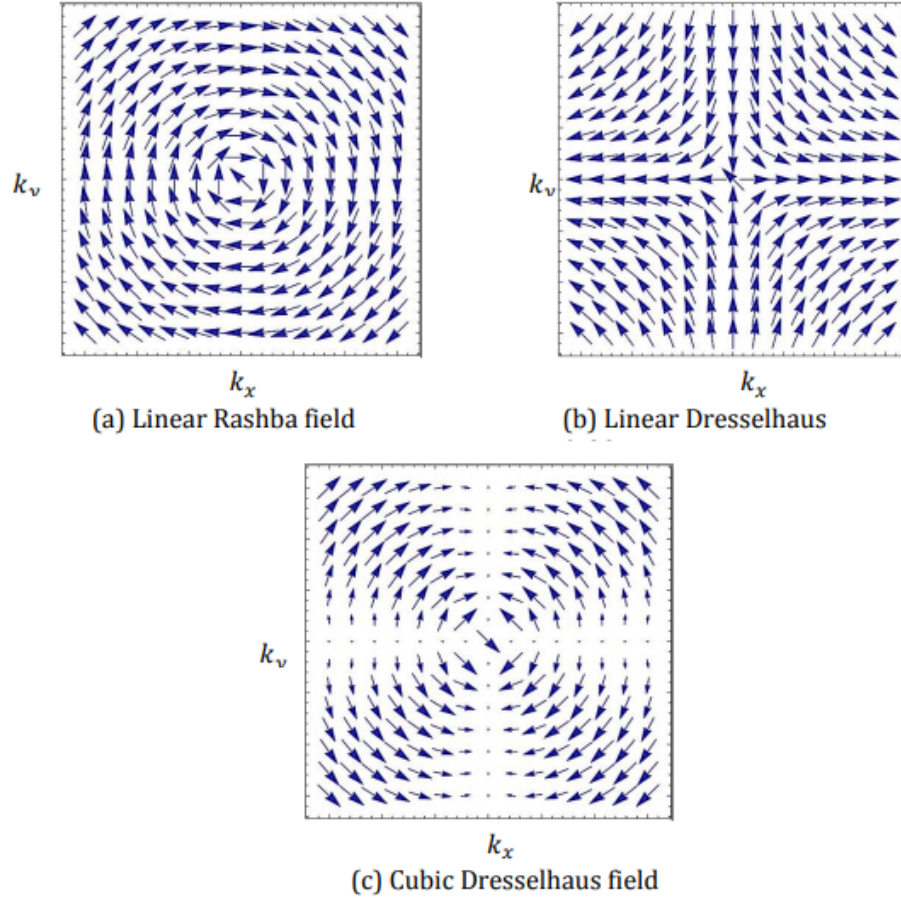


Figure 2.4: Schematic sketches of spin orientation due to Rashba and Dresselhaus effects. Here k_x is chosen to be $[010]$, k_y the $[100]$ crystal direction and z is along $[001]$

2.3 Magnetotransport in 2DEG

Magneto-transport is basically transport of electrons in semiconductors and metals in the company of a magnetic field. Restriction in the motion of electrons in a two dimensional plane (e.g 2DEG) in the company of magnetic field, will result in the most surprising and wonderful phenomenon known as Hall effect. The Hall effect was found more than ten decades ago, and has since become a generally utilized tool for considering the transport properties of materials, just as the reason for countless mechanical applications[1, 9]. Magnetotransport is an amazing and advantageous procedure to analyze 2DEG.

2.3.1 The Drude Model and the Hall effect

When applying an electric and/or magnetic field to a material the electrons or holes within that material will experience a force. Treating the carriers as though they had an effective mass m^* , a time between scattering events τ and considering the total force on the particles due to the externally applied fields results in the Drude Model [38]:

$$m^* \left(\frac{d\mathbf{v}}{dt} + \frac{\mathbf{v}}{\tau} \right) = q(\mathbf{E} + (\mathbf{v} \times \mathbf{B})) \quad (2.6)$$

where

\mathbf{v} =velocity of the carriers,

q =electronic charge,

\mathbf{E} = Electric field

\mathbf{B} = magnetic fields.

For a given carrier type of mass m^* the current density \mathbf{J} can be related to the

to the electric field via the relationship

$$\mathbf{E} = \rho \mathbf{J} \quad (2.7)$$

where ρ is the resistivity tensor. For a 2D carrier gas (2DCG) in the xy - plane with a magnetic field applied along z -axis, as in Fig. 2.5. ρ is given by the 2x2 matrix

$$\rho = \begin{bmatrix} \rho_{xx} & \rho_{xy} \\ \rho_{yx} & \rho_{yy} \end{bmatrix} \xrightarrow{\text{Onsager}} \rho = \begin{bmatrix} \rho_{xx} & \rho_{xy} \\ -\rho_{xy} & \rho_{xx} \end{bmatrix} \quad (2.8)$$

where it has been assumed that there is no current flowing in the z -direction ($J_z = 0$) and the electric fields in the y and z directions are equal to zero. Assuming Onsager reciprocity the, argument on the left side of Eq. 2.8 undergoes the transformation shown by the arrow [39]. Experimentally the transverse and longitudinal voltages, V_{xy} and V_{xx} respectively, are measured as shown in Fig. 2.5

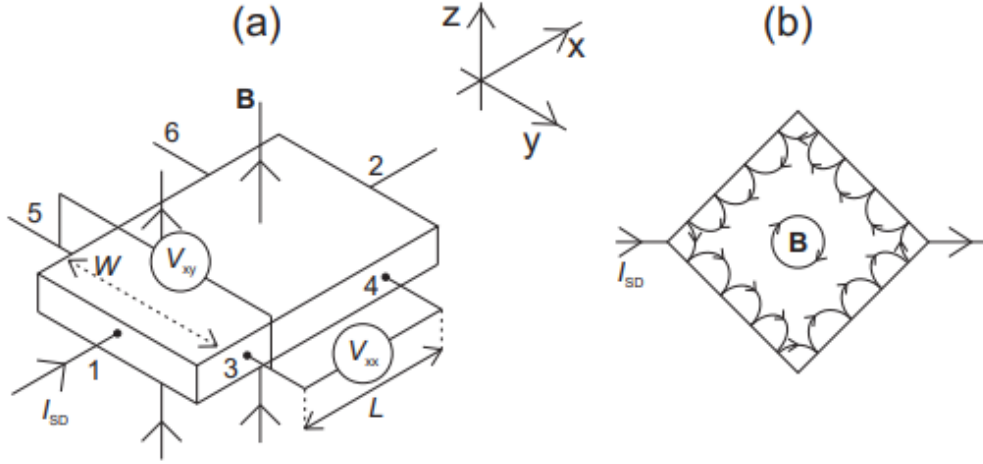


Figure 2.5: (a) Measurement setup for the Hall effect with a sample of width W and length L . The Hall voltage V_{XY} can be measured between probes 3 and 5 or 4 and 6. (b) Plan view of (a) with the voltage probes removed and the current path of the charge carriers with the effects of magnetic field.[40]

These quantities allow the carrier density and mobility to be calculated via the relations

$$\rho_{xx} = \frac{WV_{xx}}{LI} = \frac{1}{n_s e \mu}, \quad \rho_{xy} = \frac{WV_{xy}}{LI} = \frac{B}{n_s e} \quad (2.9)$$

This, however, is not the entire picture as any misalignment between the voltage probes must be taken into account as these would lead to errors when measuring V_{xy} . Using Eqs 2.6, 2.7 and 2.8 it can be shown that when the magnetic field is reversed ρ_{xx} and ρ_{xy} are respectively even and odd functions

$$\begin{aligned} \rho_{xx}(+B) &= \rho_{xx}(-B) \\ \rho_{xy}(+B) &= -\rho_{xy}(-B) \end{aligned} \quad (2.10)$$

thus

$$\rho_{xx}(+B) = \frac{W}{2L} (R_{xx}(+B) + R_{xx}(-B)) \quad (2.11)$$

$$\rho_{xy}(+B) = \frac{1}{2} (R_{xy}(+B) - R_{xy}(-B)) \quad (2.12)$$

Although this method can account to a certain degree for the inclusion of R_{xx} in the measured R_{xy} signal, it cannot fully remove its presence under certain conditions. These conditions are present at low carrier densities where ρ_{xx} will be large and magnetic fields where ρ_{xy} becomes similar in magnitude to ρ_{xx} . This introduces a high degree of noise in the measured R_{xy} signal making it more difficult to extract an accurate value of the carrier density using this method [38].

Eq. 2.9 agrees well with Hall's original measurements in 1879. [41]. However, later they were found to need modifying at lower temperatures where the quantum Hall effect appears. It is also possible to determine carrier densities via the quantum Hall effect without the need to resort to Eqs. 2.10 through 2.12.

2.3.2 The Integer Quantum Hall Effect (QHE)

In confined 2D systems, a plateau in Hall voltage occurs when the Fermi energy is halfway between two adjacent Landau levels. At this point, the DOS, and hence the longitudinal resistivity, is zero. The transverse resistivity is given as

$$R_{xy} = \frac{h}{e^2} \frac{1}{\nu}$$

where $\nu = \frac{hn_2D}{eB_2}$ is the filling factor. This quantization in the longitudinal resistivity is known as the integer quantum Hall effect. This effect was apprehensively predicted by Ando et al. in 1975 [42] and was unexpectedly discovered and reported by von

Klitzing in 1980 [43]. The main results of that study are repeated in figure 2-12

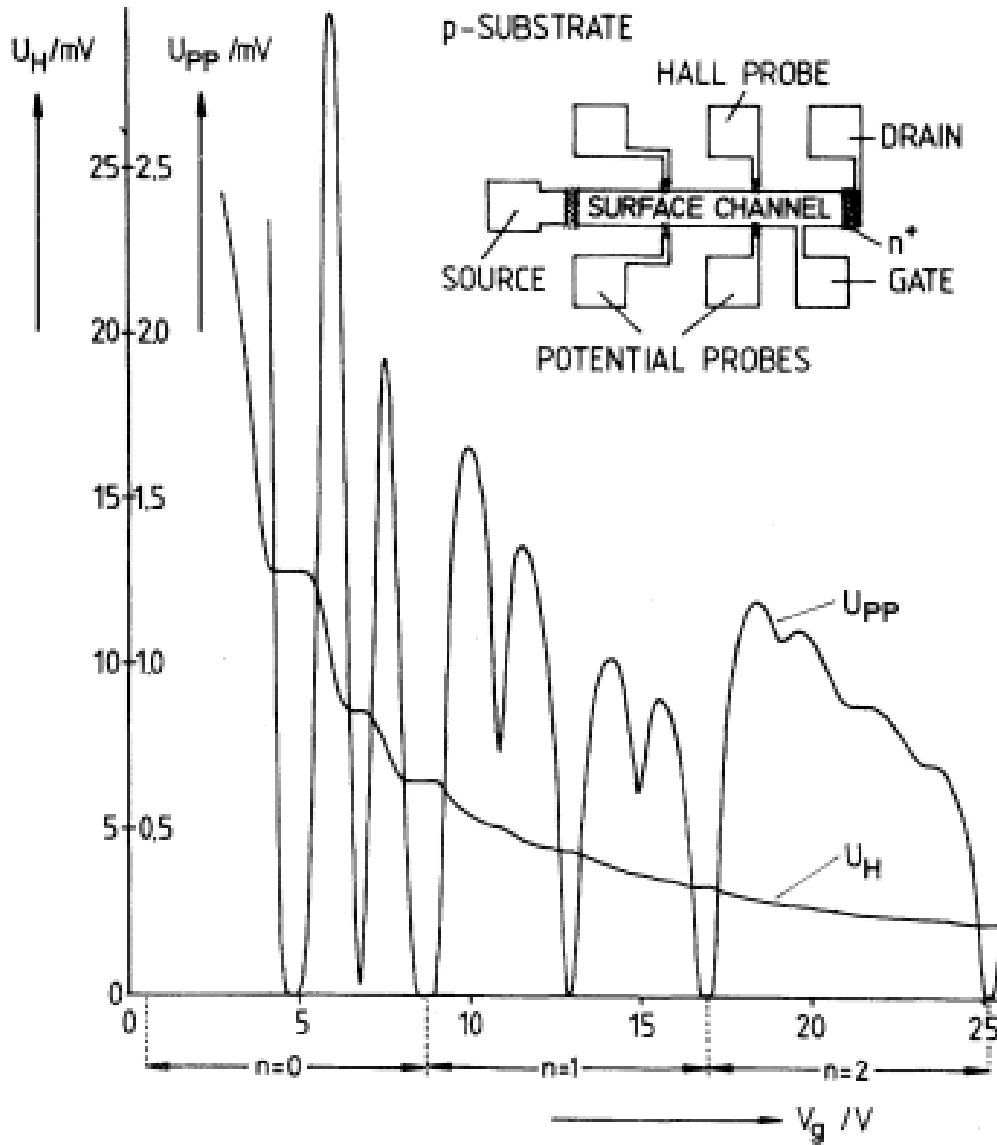


Figure 2.6: From [43]. The voltage drop U_{PP} and the Hall voltage U_H between the probes (where U_{PP} is equivalent to V_{xx} in figure 2-10) are both plotted as a function of the gate voltage V_g . Troughs and plateaus, signatures of the QHE, can be clearly seen in U_{PP} and U_H respectively.

The plateaus in V_{xy} and troughs in V_{xx} appear for the following reasons. Consider an SiMOSFET hosting a 2DEG of constant density. At zero magnetic field the density of states of this 2D system is a constant function of energy given by

$$g_{2D} = \frac{m^*m_0}{\pi h^2}$$

where

m^* = effective mass of carriers

m_0 = free electron mass[38] (Fig. 2.6(a)).

Applying a magnetic field causes the electrons to act like simple harmonic oscillators with energies E_n where n is an integer. The frequency with which the carriers orbit the magnetic flux lines is given by the cyclotron frequency $\omega_c = eB/m^*$. [38]. The effect of this on the DOS is shown in Figs. 2.6(b) and 2.6(c). As the magnetic field increases the Landau Levels move relative to E_F as the magnetic field is increased [38]. When the Fermi level be placed in a gap, as it does in Fig. 2.6(c) the movement of electrons to the new states becomes impossible and no scattering occurs. As a result of this the transport through the MOSFET is dissipationless and V_{xx} goes to zero. Additionally, the plateaus in V_{xy} appear as the edge currents in the Hall bar become quantised in units of $Ih/2e^2$. Note that although the above argument has assumed a fixed Fermi energy and electron density, the same effect can also appear for a fixed magnetic field and changing carrier density. The electron density would be altered by manipulating the gates of the device.

All of the carriers may occupy a single Landau level. In this instance the ratio of the total carrier density to the density within a Landau level is equal to one. This ratio is given by $\nu = n_n/(eB/h)$ where ν is the filling factor, n_s is the carrier

density and (eB/h) is the density of carriers in the Landau level. The effects of spin splitting on the SdH oscillations are discussed after considering the effects of the magnetic field on the carrier momentum.

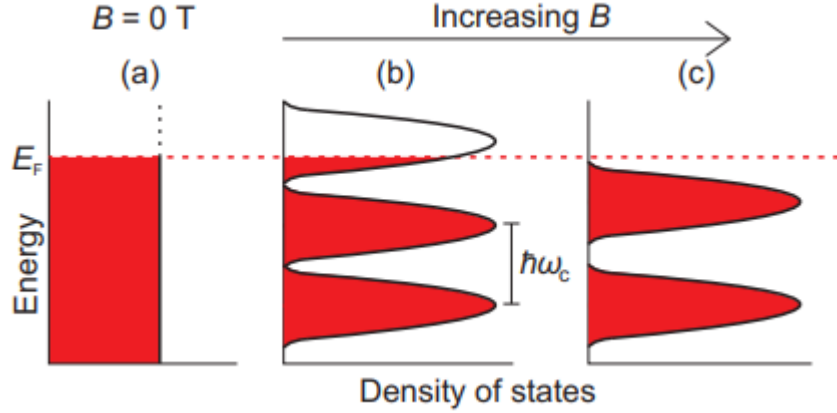


Figure 2.7: : (a) At zero magnetic field ($B = 0$ T) the 2D DOS remains constant with increasing energy. With the increase in magnetic field, available states form group into Landau levels that are separated by the cyclotron energy as shown in (b) and (c).[40]

With the effects of magnetic field the momentum of the carriers becomes $(p - eA)$ where A is defined as magnetic vector potential. Using the Landau gauge for the magnetic vector potential gives $A_y = Bx, A_x = 0$.[44]. Utilising these and considering a single particle, the SWE can be written

$$\frac{(-i\hbar\nabla - e\mathbf{A})^2}{2m^*}\Psi = E_n\Psi$$

where the potential has been set zero and Ψ is the wavefunction of the carriers in

the xy -plane. This results in the energies E_n

$$E_n = \left(n + \frac{1}{2} \right) \hbar \omega_c$$

where $\omega_c = eB/m^*$ is the cyclotron frequency. Plotting E_n as a function of B produces a fan diagram (figure 2 – 14).

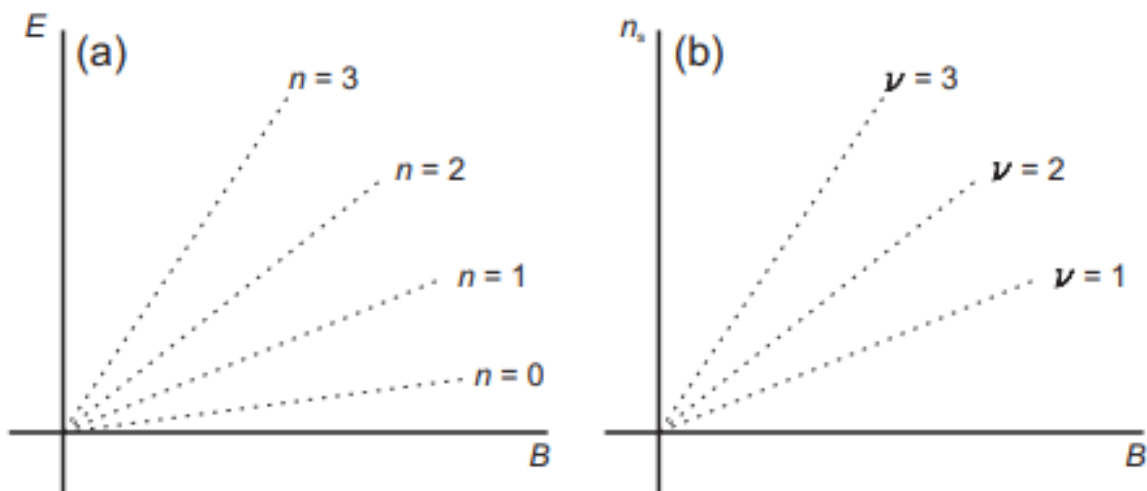


Figure 2.8: : (a) Fan diagram of first four E_n Plots (b) replacing vertical axis of energy with the sheet density.[40]

2.3.3 Shubnikov-de Haas Oscillations

With increasing magnetic field B_z , the separation between the Landau levels increases and the Landau levels pass through E_F . However, since the 2D density is constant, the Fermi energy and DOS oscillate with B_z . The Fermi energy follows each Landau level as each level depopulates. Once a Landau level is depopulated, the Fermi energy drops to the next Landau level. The oscillations of the DOS

at Fermi energy is what give rise to the SdH oscillations, where the longitudinal magnetoresistance oscillates as a function of magnetic field. When the Fermi energy is exactly in the middle of two Landau levels, the DOS is zero and so is the resistance. Conversely, when the Fermi energy coincides with a Landau level the DOS is at maximum and the resistance is finite. Therefore, for a given 2D density n_{2D} as the magnetic field is varied, the DOS oscillates periodically in $(1/B_z)$ such that

$$n_{2D} = \frac{2e}{h} \frac{\Delta n}{\Delta (1/B_z)_n} \quad (2.13)$$

where Δn is the difference in index between two adjacent Landau levels and $\Delta (1/B_z)_n$ is the spacing in $1/B_z$ corresponding to two adjacent magnetoresistance peaks. According to the Einstein relation, the conductivity of a 2D system is proportional to the DOS. Consequently, the oscillations in the DOS are manifested in the conductivity of the 2D system. Furthermore, since

$$\sigma = \begin{pmatrix} \sigma_{xx} & \sigma_{xy} \\ -\sigma_{xy} & \sigma_{xx} \end{pmatrix} = \rho^{-1} = \begin{pmatrix} \rho_{xx} & -\rho_{xy} \\ \rho_{xy} & \rho_{xx} \end{pmatrix}$$

we have:

$$\rho_{xx} = \frac{\sigma_{xx}}{\sigma_{xx}^2 + \sigma_{xy}^2}$$

$$\rho_{xy} = \frac{\sigma_{xy}}{\sigma_{xx}^2 + \sigma_{xy}^2}$$

When E_F does not coincide with a Landau level, $\sigma_{xx} \rightarrow 0$ and $\rho_{xx} \rightarrow 0$. Conversely, when E_F coincides with a Landau level, σ_{xx} is a maximum, and so is ρ_{xx} . Therefore, Shubnikov-de Haas oscillations can be seen as oscillations in ρ_{xx}

By using Eq. 2.13, if Δn and $\Delta (1/B_z)_n$ are both known, the density n_{2D} can be deduced. This result can be generalized for systems with a multi-subband occu-

pancy. When there are two occupied subbands with differing effective masses (i.e. in the case of a 2D system with finite spin-orbit interactions), the SdH oscillations show a beating pattern as each subband of population n_i gives rise to oscillations of period $\Delta(1/B_z)_n = (1/h)(1/n_e)$. The population of the individual subband can be extracted by performing Fourier transform to the SdH traces, or by counting the periodic Landau level population/depopulation. Typical experimental results for Shubnikovde Haas oscillations and Hall resistivity are shown in Fig. 2.9

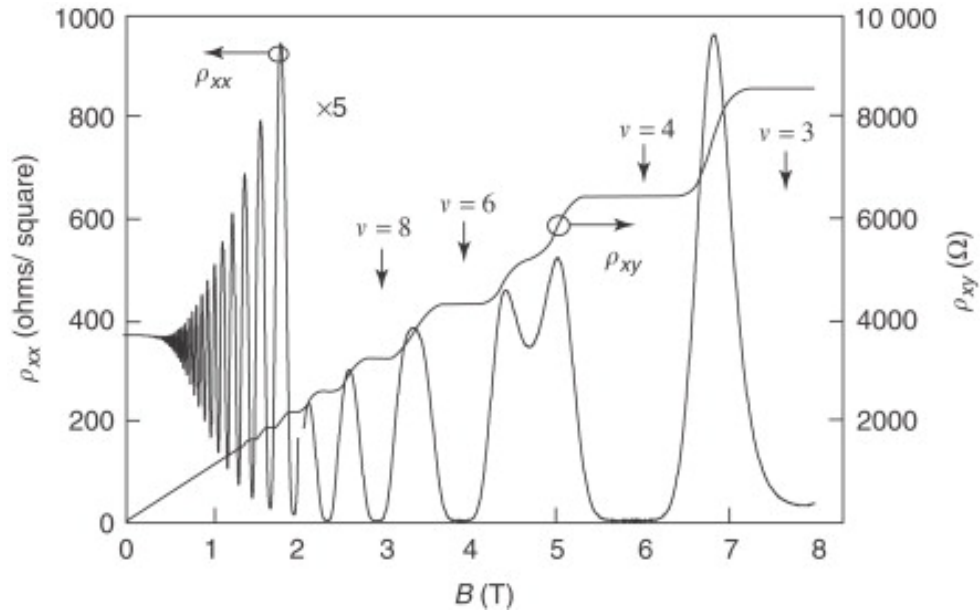


Figure 2.9: : Hall effect and SdH oscillations in a modulation-doped heterojunction of $GaAs/Ga_{0.7}Al_{0.3}As$ measured at 1.18 K. Electron density measured as $5.6 \times 10^{15} m^{-2}$ and mobility $15.3 m^2 (Vs)^{-1}$ [45].

2.4 Single Particle Picture of 2DEG

2.4.1 Landau Quantization

Classically, when an electron moves in a magnetic field then it experiences a Lorentz force $\mathbf{F} = -e[\mathbf{E} + \mathbf{v} \times \mathbf{B}]$, which in the absence of electric field would be $\mathbf{F} = -e(\mathbf{v} \times \mathbf{B})$. This force results in the circular motion of electron for which the Lorentz force provides centripetal acceleration.

$$\frac{v^2}{r} = \frac{-evB}{m} \quad (2.14)$$

and hence

$$\mathbf{r} = \frac{m\mathbf{v}}{-e\mathbf{B}}$$

This is the cyclotron or Larmour radius and the cyclotron frequency, that is independent of radius, can be written as

$$\omega = \frac{-e\mathbf{B}}{m}$$

Similarly, energy of the system can be written as

$$\mathbf{E} = \frac{mv^2}{2} = \frac{1}{2}m\mathbf{r}^2\omega^2$$

Quantum mechanically, these cyclotron orbits are quantized i.e. charge particle can occupy only those orbits which have discrete values of energy. These discrete levels are called Landau levels and quantization is known as Landau quantization.

2.4.2 Kinetic term

For a two dimensional system of a particle in the presence of a magnetic field \mathbf{B} that is in the z -direction i.e. $\mathbf{B} = \begin{pmatrix} 0 \\ 0 \\ B \end{pmatrix}$, we have Lagrangian

$$L = \frac{1}{2}m(\dot{x}^2 + \dot{y}^2) + e\mathbf{A} \cdot \mathbf{v} \quad (2.15)$$

where \mathbf{A} is the vector potential and $\mathbf{v} = \dot{x}\hat{i} + \dot{y}\hat{j}$ is the velocity of particle. For given a magnetic field, there is a gauge freedom in the choice of the vector potential. To make our calculations simple we consider Landau gauge in which,

$$\mathbf{A} = (0, Bx, 0)$$

As magnetic field is in the z direction and vector potential is in the y -direction, the Lagrangian can be written as,

$$L = \frac{1}{2}m(\dot{x}_i^2 + \dot{y}_i^2) + e|A|\dot{y}$$

From the Lagrangian, the canonical momenta can be easily determined using

$$\begin{aligned} P_x &= \frac{\partial L}{\partial \dot{x}} = m\dot{x} \\ \Rightarrow \dot{x} &= \frac{P_x}{m} \end{aligned}$$

and

$$P_y = \frac{\partial L}{\partial \dot{y}} = m\dot{y} + eA_y$$

$$\Rightarrow \dot{y} = \frac{(P_y + eA_y)}{m}$$

We can find out Hamiltonian easily by using all the above parameters

$$H = \sum_i P_i \dot{q}_i - L$$

$$\Rightarrow H = P_x \dot{x} + P_y \dot{y} - L$$

$$H = P_x \left(\frac{P_x}{m} \right) + P_y \frac{(P_y + eA_y)}{m} - \frac{1}{2} m ((P_x m)^2 + (P_y + eA_y)^2) + eA(P + eA_y)$$

$$H = \frac{P_x^2}{2m} + (P_y + eA_y) \frac{(P_y + eA_y)}{m} - \frac{(P_y + eA_y)^2}{2m}$$

$$H = \frac{P_x^2}{2m} + \frac{(P_y + eA_y)^2}{2m} \tag{2.16}$$

Using $A_y = Bx$ we get,

$$H = \frac{P_x^2}{2m} + \frac{(P_y + eBx)^2}{2m}$$

$$H = \frac{P_x^2}{2m} + \frac{e^2 B^2}{2m} \left(\frac{P_y}{eB} + x \right)^2$$

It can be seen from above equation that y does not appear in this Hamiltonian which means that it is a cyclic coordinate implying that, P_y is conserved. In other words we can say that the Hamiltonian commutes with P_y and we can use $x_0 = \frac{P_y}{eB}$ and $\omega = \frac{eB}{m}$ to get,

$$H = \frac{P_x^2}{2m} + \frac{1}{2} m \omega^2 (x + x_0)^2 \tag{2.17}$$

which is similar to the Hamiltonian of simple harmonic motion restricted to move along the x axis about point x_0 . Now we have to find out the eigenfunction of this Hamiltonian. By applying Schroedinger wave equation we get,

$$\left(\frac{P_x^2}{2m} + \frac{1}{2}m\omega^2(x + x_0)^2 \right) \psi(x, y) = E\psi(x, y)$$

where $\psi(x, y)$ is an eigenfunction and we can solve this equation by using separation of variables method by considering $\psi(x, y) = \phi(x)\phi(y)$.

$$\left(\frac{P_x^2}{2m} + \frac{1}{2}m\omega^2(x + x_0)^2 \right) \phi(x)\phi(y) = E\phi(x)\phi(y)$$

As y is cyclic coordinate in this case and Hamiltonian commutes with P_y hence the $\phi(y)$ has simply the plane wave solution that is $\phi(y) = Ae^{ik_y y}$ where A is the normalization constant having value of $\frac{1}{\sqrt{L_y}}$ and L_y is the length of system in the y direction. Now all we need to do is solve for $\phi(x)$ using,

$$\frac{P_x^2}{2m} + \frac{1}{2}m\omega^2(x + x_0)^2 \phi(x) = E\phi(x) \quad (2.18)$$

Let us introduce $\xi \equiv \sqrt{\frac{m\omega}{\hbar}}(x + x_0)$ and $l \equiv \sqrt{\frac{\hbar}{m\omega}}$. To solve this we temporarily make the change $(x + x_0) \rightarrow x$ so, $\xi = \sqrt{\frac{m\omega}{\hbar}}x$. To quantize Hamiltonian we construct a and a^\dagger

$$a^\dagger = \frac{1}{\sqrt{2m\hbar\omega}}(-i\hat{p} + m\omega x)$$

$$a = \frac{1}{\sqrt{2m\hbar\omega}}(i\hat{p} + m\omega x)$$

as $\hat{p}_x = -i\hbar\frac{\delta}{\delta x}$ so we can write a^\dagger and a in the form of ξ ,

$$\begin{aligned} a^\dagger &= \frac{1}{\sqrt{2}}\left(\xi - \frac{\delta}{\delta x}\right) \\ a &= \frac{1}{\sqrt{2}}\left(\xi + \frac{\delta}{\delta x}\right) \end{aligned}$$

So now we can write Hamiltonian in the form of annihilation and creation operator as

$$H = \hbar\omega\left(\frac{1}{2} + a^\dagger a\right) \quad (2.19)$$

To find wave function $\phi(x)$ we first need to find out the wave function at ground state which obeys the condition, $a\phi_0 = 0$. Now by this condition we calculate the ground state wave function as

$$\begin{aligned} \left(\xi + \frac{\delta}{\delta x}\right)\phi_0 &= 0 \\ \frac{\delta\phi_0}{\delta\xi} &= -\xi\phi_0 \end{aligned}$$

By integrating above equation over the interval 0 to ϕ_0 and 0 to ξ , we get $\phi_0 = A_0 e^{-\xi^2/2}$. Through normalization we can easily get the value of normalization constant, which is $\frac{1}{(\pi)^{1/4}}$. So ground state wave function is

$$\phi_0 = \frac{1}{(\pi)^{1/4}} e^{-\xi^2/2}$$

Similarly, we can find out ϕ_1 by applying a^\dagger on the ground state as it will raise the quantum state of particle.

$$\begin{aligned}
\phi_1 &= a^\dagger \phi_0 \\
\phi_2 &= \frac{1}{\sqrt{2}} a^\dagger \phi_1 = \frac{1}{\sqrt{2}} a^\dagger a^\dagger \phi_0 = \frac{1}{\sqrt{2}} (a^\dagger)^2 \phi_0 \\
&\cdot \\
&\cdot \\
&\cdot \\
&\cdot \\
\phi_n &= \frac{1}{\sqrt{n}} (a^\dagger)^n \phi_0
\end{aligned}$$

Now by putting the value of a^\dagger and ξ and substituting the value of Hermite polynomials that is $H_n(\xi) = (-1)^n e^{\xi^2/2} \frac{d^n}{d\xi^n} e^{-\xi^2/2}$, wave function $\phi_n(x)$ becomes,

$$\phi_n(x) = \frac{1}{\sqrt{n! 2^n \pi^{1/2}}} H_n\left(\frac{x + x_0}{l}\right) e^{-(x+x_0)^2/(2l)^2}$$

Combining both the solutions i.e. $\phi(x)$ and $\phi(y)$ we can write the complete solution of eigenfunction as

$$\psi_n(x, y) = \frac{1}{\sqrt{L_y}} e^{ik_y y} \frac{1}{\sqrt{n! 2^n \pi^{1/2}}} H_n\left(\frac{x + x_0}{l}\right) e^{-(x+x_0)^2/(2l)^2} \quad (2.20)$$

In the next chapter, we are going to derive Hamiltonian for our system by applying non relativistic limit on Dirac equation. Using the same approach, we will determine the eigen values and corresponding eigenfunctions.

Chapter 3

Methodology

A 2DEG is considered in xy plane with magnetic field in z -direction. We use Landau gauge $\mathbf{A} = (-By, 0, 0)$, as a gauge freedom, in the 1e Hamiltonian. With Rashba term this Hamiltonian reads

$$H = \frac{(\mathbf{p} + e\mathbf{A})^2}{2m^*} + \frac{\alpha}{\hbar}[\boldsymbol{\sigma} \times (\mathbf{p} + e\mathbf{A})]_z + g\mu_B B\sigma_z \quad (3.1)$$

where

\mathbf{p} = electron's momentum operator,

m^* = effective mass of electron,

μ_B = Bohr magneton,

g = Zeeman factor,

$\boldsymbol{\sigma} = (\sigma_x, \sigma_y, \sigma_z)$ = spin Pauli matrix

α = strength of SOI

3.0.1 Derivation of Hamiltonian

Hamiltonian of this system can be derived from Dirac Equation

$$(i\gamma^\mu D_\mu - m)\psi = 0 \quad (3.2)$$

Where ψ is the wave function for 4-spinors, that gives a detail account for spin-1/2 particles having mass m , $\partial_\mu = \frac{\partial}{\partial x^\mu}$ are partial derivatives with the reference to space-time coordinates $x^\mu = t, x, y, z$ and γ_μ are Dirac 4×4 matrices. Using identity $D_\mu = \partial_\mu - ieA_\mu$ in above equation,we get

$$[i\gamma^\mu(\partial_\mu - ieA_\mu) - m]\psi = 0$$

$$[\gamma^\mu(i\delta_\mu - i^2eA_\mu) - m]\psi = 0$$

$$[\gamma^\mu(P_\mu + eA_\mu) - m]\psi = 0$$

As we know that momentum operator is $P_\mu = -\frac{\hbar}{i} \frac{\partial}{\partial x^\mu}$ putting in above equation,we get

$$[\gamma^\mu\{(-\frac{\hbar}{i} \frac{\partial}{\partial x^\mu}) + eA_\mu\} - m]\psi = 0$$

$$[\gamma^\mu\{(\frac{\partial}{\partial x^\mu}) - \frac{i}{\hbar}eA_\mu\} + \frac{i}{\hbar}m]\psi = 0$$

introducing a constant $k = \frac{m}{\hbar}$

$$[\gamma^\mu\{(\frac{\partial}{\partial x^\mu}) - \frac{i}{\hbar}eA_\mu\} + ik]\psi = 0 \quad (3.3)$$

Taking its adjoint we get,

$$\begin{aligned}
\left(\frac{\partial}{\partial x^\mu} + \frac{i}{\hbar}eA_\mu\right)\psi^\dagger(\gamma^\mu)^\dagger - ik\psi^\dagger &= 0 \\
(\gamma^\mu)^\dagger\gamma^0 &= \gamma^0\gamma^\mu \\
\bar{\psi} &= \psi^\dagger\gamma^0 \\
\left(\frac{\partial}{\partial x^\mu} + \frac{i}{\hbar}eA_\mu\right)\bar{\psi}(\gamma^\mu) - ik\bar{\psi} &= 0
\end{aligned}$$

starting from equation (3.3)

$$[\gamma^0\left\{\left(\frac{\partial}{\partial x^0} - \frac{i}{\hbar}eA_0\right) + \gamma^i\left\{\left(\frac{\partial}{\partial x^i} - \frac{i}{\hbar}eA_i\right) + ik\right\}\right]\psi = 0$$

multiplying both sides by $i\hbar\gamma^0$ and $(\gamma^0)^2 = 1$

$$[i\hbar\left\{\left(\frac{\partial}{\partial x^0} - \frac{i}{\hbar}eA_0\right) + i\hbar\gamma^0\gamma^i\left\{\left(\frac{\partial}{\partial x^i} - \frac{i}{\hbar}eA_i\right) + i^2\hbar\gamma^0k\right\}\right]\psi = 0$$

taking $x^0 = t$

$$i\hbar\frac{\delta\psi}{\delta t} = -eA_0\psi - i\hbar\gamma^0\gamma^i\frac{\partial\psi}{\partial x^i} - e\gamma^0\gamma^iA_i\psi + \gamma^0m\psi$$

now this equation has the form of SWE

$$i\hbar\frac{\partial\psi}{\partial t} = H\psi$$

By comparing with Schrodinger Wave equation we have Hamiltonian

$$\begin{aligned}
 H &= -eA_0 - i\hbar\gamma^0\gamma^i\frac{\partial}{\partial x^i} - e\gamma^0\gamma^iA_i + \gamma^0m \\
 H &= \gamma^0\gamma^i(-i\hbar\frac{\partial}{\partial x^i} - eA_i) - eA_0 + \gamma^0m \\
 H &= -\gamma^i\gamma^0(P_i + eA_i) - eA_0 + \gamma^0m
 \end{aligned}$$

introducing $\pi_i = (P_i + eA_i)$ and putting matrices $\gamma^i\gamma^0$

$$\begin{aligned}
 H &= - \begin{pmatrix} 0 & \sigma_i \\ -\sigma_i & 0 \end{pmatrix} \begin{pmatrix} \pi_i & 0 \\ 0 & -\pi_i \end{pmatrix} + \begin{pmatrix} -eA_0 & 0 \\ 0 & -eA_0 \end{pmatrix} + \begin{pmatrix} m & 0 \\ 0 & -m \end{pmatrix} \\
 H - m &= \begin{pmatrix} 0 & \boldsymbol{\sigma} \cdot \boldsymbol{\pi} \\ -\boldsymbol{\sigma} \cdot \boldsymbol{\pi} & 0 \end{pmatrix} + \begin{pmatrix} -eA_0 & 0 \\ 0 & -eA_0 \end{pmatrix} + \begin{pmatrix} 0 & 0 \\ 0 & -2m \end{pmatrix} \\
 H - m &= \begin{pmatrix} -eA_0 & \boldsymbol{\sigma} \cdot \boldsymbol{\pi} \\ \boldsymbol{\sigma} \cdot \boldsymbol{\pi} & -eA_0 - 2m \end{pmatrix} \tag{3.4}
 \end{aligned}$$

Now we consider the Dirac spinor

$$\psi(x, t) = e^{-imt} \begin{pmatrix} \phi \\ \xi \end{pmatrix}$$

as $i\hbar\frac{\partial\psi}{\partial t} = H\psi$

$$\begin{aligned}
i\partial_0\psi &= i\partial_0 e^{-imt} \begin{pmatrix} \phi \\ \xi \end{pmatrix} \\
e^{-imt} H \begin{pmatrix} \phi \\ \xi \end{pmatrix} &= m e^{-imt} \begin{pmatrix} \phi \\ \xi \end{pmatrix} + e^{-imt} i\partial_0 \begin{pmatrix} \phi \\ \xi \end{pmatrix} \\
i\partial_0 \begin{pmatrix} \phi \\ \xi \end{pmatrix} &= (H - m) \begin{pmatrix} \phi \\ \xi \end{pmatrix}
\end{aligned} \tag{3.5}$$

Inserting equation (3.4) into above equation,

$$i\partial_0 \begin{pmatrix} \phi \\ \xi \end{pmatrix} = \begin{pmatrix} -eA_0 & \boldsymbol{\sigma}\cdot\boldsymbol{\pi} \\ \boldsymbol{\sigma}\cdot\boldsymbol{\pi} & -eA_0 - 2m \end{pmatrix} \begin{pmatrix} \phi \\ \xi \end{pmatrix}$$

$$i\partial_0\phi = eA_0 + \boldsymbol{\sigma}\cdot\boldsymbol{\pi}\xi \tag{3.6}$$

$$i\partial_0\xi = \boldsymbol{\sigma}\cdot\boldsymbol{\pi}\phi - (2m - eA_0)\xi \tag{3.7}$$

If the kinetic energy and field interaction energies are small enough as compared to the rest mass so from eq. (3.7)

$$\begin{aligned}
(2m - eA_0)\xi &= \boldsymbol{\sigma}\cdot\boldsymbol{\pi}\phi \\
\xi &= \frac{\boldsymbol{\sigma}\cdot\boldsymbol{\pi}\phi}{(2m - eA_0)} \\
\frac{1}{2m(1 - eA_0/2m)} &= \frac{(1 - eA_0/2m)^{-1}}{2m}
\end{aligned}$$

so we can write ξ as

$$\xi = \frac{1}{2m} \left(1 + \frac{eA_0}{2m}\right) \boldsymbol{\sigma}\cdot\boldsymbol{\pi}\phi$$

eq.(3.6) becomes

$$i\partial_0\phi = \frac{1}{2m}(\boldsymbol{\sigma}\cdot\boldsymbol{\pi})(\boldsymbol{\sigma}\cdot\boldsymbol{\pi}) + \frac{e}{4m^2}(\boldsymbol{\sigma}\cdot\boldsymbol{\pi})A_0(\boldsymbol{\sigma}\cdot\boldsymbol{\pi}\phi) + eA_0\phi \quad (3.8)$$

solving the operator

$$(\boldsymbol{\sigma}\cdot\boldsymbol{\pi})(\boldsymbol{\sigma}\cdot\boldsymbol{\pi}) = \pi^2 + i\boldsymbol{\sigma}\cdot(\boldsymbol{\pi} \times \boldsymbol{\pi})$$

where

$$\begin{aligned} \pi^2 &= (\mathbf{P} + e\mathbf{A})^2 \\ (\boldsymbol{\pi} \times \boldsymbol{\pi})\phi &= \frac{e}{i}[(\boldsymbol{\nabla} \times \mathbf{A})\phi + (\boldsymbol{\nabla}\phi) \times \mathbf{A} + \mathbf{A} \times ((\boldsymbol{\nabla}\phi))] \\ &= \frac{e}{i}\mathbf{B}\phi \end{aligned}$$

first term of eq. (3.8) can be written as

$$\begin{aligned} \frac{1}{2m}(\boldsymbol{\sigma}\cdot\boldsymbol{\pi})(\boldsymbol{\sigma}\cdot\boldsymbol{\pi}) &= \frac{1}{2m}(\mathbf{P} + e\mathbf{A})^2 + \frac{e}{2m}\boldsymbol{\sigma}\cdot\mathbf{B} \\ &= \frac{1}{2m}(\mathbf{P} + e\mathbf{A})^2 + g\mu_B\boldsymbol{\sigma}\cdot\mathbf{B} \end{aligned} \quad (3.9)$$

here $\mu_B = \frac{e}{2m}$, taking $\hbar = 1$. solving second part of eq. (3.8)

$$\begin{aligned} \frac{e}{4m^2}(\boldsymbol{\sigma}\cdot\boldsymbol{\pi})A_0(\boldsymbol{\sigma}\cdot\boldsymbol{\pi}\phi) &= \frac{e}{4m^2}\sigma^i\pi^i A_0\sigma^j\pi^j \\ &= \frac{e}{4m^2}\sigma^i\sigma^j A_0\pi^i\pi^j \\ &= \frac{e}{4m^2}(\partial^{ij} + i\varepsilon^{ijk}\sigma^k)\pi^i A_0\pi^j \\ &= \frac{e}{4m^2}\pi^i A_0\pi^j + i\varepsilon^{ijk}\sigma^k\pi^i A_0\pi^j \end{aligned}$$

$\pi^i A_0 \pi^j$ term have no contribution in non-relativistic case since it contributes P^2/m^2 , so we consider second term only

$$i\varepsilon^{ijk}\sigma^k\pi^i A_0\pi^j = i\varepsilon^{ijk}\sigma^k[\pi^i, A_0]\pi^j + i\varepsilon^{ijk}\sigma^k A_0\pi^i\pi^j$$

second term would vanish and ignoring the second and third terms of potential

$$\begin{aligned} &= i\varepsilon^{ijk}\sigma^k[P^i, A_0]P^j \\ &= \boldsymbol{\sigma}(\nabla\phi \times \mathbf{P}) \\ &\quad \nabla\phi = \phi' \frac{\mathbf{r}}{r} \\ &= \frac{e}{4m} \frac{1}{r} \phi' \boldsymbol{\sigma} \cdot (\mathbf{r} \times \mathbf{P}) \\ &= \alpha(\boldsymbol{\sigma} \cdot \mathbf{L}) \end{aligned}$$

combining Eq. (3.8), (3.9) and ignoring the term eA_0 due to absence of external electric field, we get Hamiltonian as

$$H = \frac{1}{2m}(\mathbf{P} + e\mathbf{A})^2 + g\mu_B \boldsymbol{\sigma} \cdot \mathbf{B} + \alpha(\boldsymbol{\sigma} \cdot \mathbf{L}) \quad (3.10)$$

3.0.2 Eigenstates and Eigenvalues

By using Landau wave function excluding spin orbit interaction as a basis our relevant eigen wavefunction can be expressed as(Hamiltonian commutes with k_x)

$$\psi_{\mathbf{k}}(\mathbf{r}) = \frac{e^{ik_x x}}{\sqrt{L_x}} \sum_n \phi(y - y_c) C_n^\sigma |\sigma\rangle$$

$$= \frac{e^{ik_x x}}{\sqrt{L_x}} \sum_n \phi(y - y_c) \begin{pmatrix} C_n^+ \\ C_n^- \end{pmatrix} \quad n = 0, 1, 2, \dots \quad (3.11)$$

Here

L_x = length of system in the x -direction

$\phi_n(y - y_c) = \frac{1}{\sqrt{\sqrt{\pi} 2^n n! l_c}} e^{(y-y_c)^2/2l_c^2} H_n\left(\frac{y-y_c}{l_c}\right)$ = Harmonic oscillator function

$l_c = \sqrt{\frac{\hbar}{m\omega_c}}$ = cyclotron orbit's radius centered at $y_c = l_c^2 k_x$

$\omega_c = eB/m$ = cyclotron frequency

n = index of Landau level

$|\sigma\rangle$ = electron spin which is written as column vector

$|\sigma\rangle = \begin{pmatrix} 1 \\ 0 \end{pmatrix}$ = for spin up and $|\sigma\rangle = \begin{pmatrix} 0 \\ 1 \end{pmatrix}$ = for spin down Now we have Hamiltonian

and wave function in matrix form as

$$H = \begin{pmatrix} \frac{\hbar^2}{2ml_c^2}(y - y_c)^2 + \frac{p_y^2}{2m} + g\mu B & \frac{\alpha}{\hbar} p_y - \frac{i\alpha}{l_c^2}(y - y_c) \\ \frac{\alpha}{\hbar} p_y + \frac{i\alpha}{l_c^2}(y - y_c) & \frac{\hbar^2}{2ml_c^2}(y - y_c)^2 + \frac{p_y^2}{2m} - g\mu B \end{pmatrix}$$

$$\psi_{\mathbf{k}}(\mathbf{r}) = \begin{pmatrix} \frac{e^{ik_x x}}{\sqrt{L_x}} \sum_n \phi(y - y_c) C_n^+ \\ \frac{e^{ik_x x}}{\sqrt{L_x}} \sum_n \phi(y - y_c) C_n^- \end{pmatrix}$$

Substituting into Schrodinger wave equation $H\psi = E\psi$

$$\begin{pmatrix} \frac{\hbar^2}{2ml_c^2}(y - y_c)^2 + \frac{p_y^2}{2m} + E_+ & \frac{\alpha}{\hbar} p_y - \frac{i\alpha}{l_c^2}(y - y_c) \\ \frac{\alpha}{\hbar} p_y + \frac{i\alpha}{l_c^2}(y - y_c) & \frac{\hbar^2}{2ml_c^2}(y - y_c)^2 + \frac{p_y^2}{2m} + E_- \end{pmatrix} \begin{pmatrix} \frac{e^{ik_x x}}{\sqrt{L_x}} \sum_n \phi_n(y - y_c) C_n^+ \\ \frac{e^{ik_x x}}{\sqrt{L_x}} \sum_n \phi_n(y - y_c) C_n^- \end{pmatrix} = 0$$

where $E_+ = g\mu B - E$ and $E_- = -g\mu B - E$. By multiplying both matrices we get

$$\left(\frac{\hbar^2}{2ml_c^4}(y-y_c)^2 + \frac{p_y^2}{2m} + E_+\right)\left(\frac{e^{ik_x x}}{\sqrt{L_x}}\Sigma_n\phi_n(y-y_c)C_n^+\right) + \left(\frac{\alpha}{\hbar}p_y - \frac{i\alpha}{l_c^2}(y-y_c)\right)\left(\frac{e^{ik_x x}}{\sqrt{L_x}}\Sigma_n\phi_n(y-y_c)C_n^-\right) = 0 \quad (3.12)$$

$$\left(\frac{\alpha}{\hbar}p_y + \frac{i\alpha}{l_c^2}(y-y_c)\right)\left(\frac{e^{ik_x x}}{\sqrt{L_x}}\Sigma_n\phi_n(y-y_c)C_n^+\right) + \left(\frac{\hbar^2}{2ml_c^4}(y-y_c)^2 + \frac{p_y^2}{2m} + E_-\right)\left(\frac{e^{ik_x x}}{\sqrt{L_x}}\Sigma_n\phi_n(y-y_c)C_n^-\right) \quad (3.13)$$

using $p_y = -i\hbar\frac{\partial}{\partial y}$

$$\begin{aligned} &\frac{\hbar^2}{2ml_c^4}(y-y_c)^2\Sigma_n\phi_n(y-y_c)C_n^+ - \frac{\hbar^2}{2m}\Sigma_n\phi_n''(y-y_c)C_n^+ + E_+\Sigma_n\phi_n(y-y_c)C_n^+ \\ &- \alpha\Sigma_n\phi_n'(y-y_c)C_n^- - \frac{\alpha}{l_c^2}(y-y_c)\Sigma_n\phi_n(y-y_c)C_n^- = 0 \end{aligned} \quad (3.14)$$

$$\begin{aligned} &-i\alpha\Sigma_n\phi_n'(y-y_c)C_n^+ + \frac{i\alpha}{l_c^2}(y-y_c)\Sigma_n\phi_n(y-y_c)C_n^+ + \frac{\hbar^2}{2ml_c^4}(y-y_c)^2\Sigma_n\phi_n(y-y_c)C_n^- \\ &- \frac{\hbar^2}{2m}\Sigma_n\phi_n''(y-y_c)C_n^- + E_-\Sigma_n\phi_n(y-y_c)C_n^- = 0 \end{aligned} \quad (3.15)$$

solving Eq. (3.14) first by using identities

$$\begin{aligned} \psi_n''(x) &= (-2n - 1 + x^2)\psi_n(x) \\ \psi'(x) &= \sqrt{\frac{n}{2}}\psi_{n-1}(x) - \sqrt{\frac{n+1}{2}}\psi_{n+1}(x) \\ x\psi_n(x) &= \sqrt{\frac{n}{2}}\psi_{n-1}(x) + \sqrt{\frac{n+1}{2}}\psi_{n+1}(x) \end{aligned}$$

we get

$$[\hbar\omega_c(n+1/2) + E_+]\phi_n(y-y_c)C_n^+ - \frac{i\alpha}{l_c}\sqrt{2n}\phi_{n-1}(y-y_c)C_n^- = 0 \quad (3.16)$$

similarly by solving Eq. (3.15) we get

$$\frac{i\alpha}{l_c} \sqrt{2(n+1)} \phi_{n+1}(y-y_c) C_n^+ + [\hbar\omega_c(n+1/2) + E_-] \phi_n(y-y_c) C_n^- = 0 \quad (3.17)$$

multiplying by $\phi_l(y-y_c)$ and integrating over y , we find the system of equations as follows (by using property of orthogonality $\int_{-\infty}^{\infty} \psi_n(x)\psi_l(x)dx = \delta_{nl}$)

$$\left\{ \begin{array}{l} [\hbar\omega_c(l+1/2) + E_+] C_l^+ - i(\alpha/l_c) \sqrt{2(l+1)} C_{l+1}^- = 0 \\ i(\alpha/l_c) \sqrt{2l} C_{l-1}^+ + [\hbar\omega_c(l+1/2) + E_-] C_l^- = 0 \end{array} \right\} \quad (3.18)$$

here $l = 0, 1, 2, 3, \dots$. We can solve this infinite system of equations by converting it into 1 or 2-dimensional secular equations with s as a new index.

$$[1/2\hbar\omega_c + E_-] C_s^- = 0, s = 0$$

$$\left(\begin{array}{cc} (s-1/2)\hbar\omega_c + E_+ & -i(\alpha/l_c)\sqrt{2s} \\ i(\alpha/l_c)\sqrt{2s} & (s+1/2)\hbar\omega_c + E_- \end{array} \right) \left\{ \begin{array}{l} C_{s-1}^+ \\ C_s^- \end{array} \right\} = 0 \quad (3.19)$$

Corresponding to ground level there is only one lowest level just like Landau level without spin orbit interaction. Energy and wave function of ground state can be written as

$$E_0 = 1/2\hbar\omega_c - g\mu_B B$$

$$\psi_0(k_x) = \frac{e^{ik_x x}}{\sqrt{L_x}} \phi_0(y-y_c) \begin{pmatrix} 0 \\ 1 \end{pmatrix}$$

By taking determinant of the matrix in Eq. (3.19) we obtain energy branches for

$s = 1, 2, 3, \dots$

$$\begin{aligned} ((s - 1/2)\hbar\omega_c + E_+)((s + 1/2)\hbar\omega_c + E_-) + (-i(\alpha/l_c)\sqrt{2s})(i(\alpha/l_c)\sqrt{2s}) &= 0 \\ E^2 - 2s\hbar\omega_c - [E_0^2 + 2s\alpha^2/l_c^2 - s^2\hbar^2\omega_c^2] &= 0 \end{aligned}$$

solving quadratic equation we get two branches of energy levels

$$E^\pm = s\hbar\omega_c \pm \sqrt{E_0^2 + 2s\alpha^2/l_c^2} \quad (3.20)$$

To find wavefunction we first need to find out the value of coefficients C_{s-1}^+ and C_s^- .

For this we solve Eq. (3.19) by substituting the values of E_+ and E_- ,

$$[(s - 1/2)\hbar\omega_c + g\mu_B B - E]C_{s-1}^+ - i(\alpha/l_c)\sqrt{2s}C_s^- = 0 \quad (3.21)$$

$$i(\alpha/l_c)\sqrt{2s}C_{s-1}^+ + [(s + 1/2)\hbar\omega_c - g\mu_B B - E]C_s^- = 0 \quad (3.22)$$

Solving Eq. (3.21) first for + branch,

$$[(s - 1/2)\hbar\omega_c + g\mu_B B - s\hbar\omega_c - \sqrt{E_0^2 + 2s\alpha^2/l_c^2}]C_{s-1}^+ - i(\alpha/l_c)\sqrt{2s}C_s^- = 0$$

$$C_{s-1}^+ = \frac{-i(\alpha/l_c)\sqrt{2s}C_s^-}{E_0 + \sqrt{E_0^2 + 2s\alpha^2/l_c^2}}$$

$$C_{s-1}^+ = -iD_s C_s^-$$

Now solving Eq. (3.22) for - branch,

$$i(\alpha/l_c)\sqrt{2s}C_{s-1}^+ + [(s + 1/2)\hbar\omega_c - g\mu_B B - s\hbar\omega_c + \sqrt{E_0^2 + 2s\alpha^2/l_c^2}]C_s^- = 0$$

$$C_s^- = \frac{-i(\alpha/l_c)\sqrt{2s}C_{s-1}^+}{E_0 + \sqrt{E_0^2 + 2s\alpha^2/l_c^2}}$$

$$C_s^- = -iD_s C_{s-1}^+$$

Now the wave function of + branch is

$$\psi_s^+(k_x) = \frac{1}{\sqrt{L_x A_s}} e^{ik_x x} \begin{pmatrix} -iD_s \phi_{s-1}(y - y_c) \\ \phi_s(y - y_c) \end{pmatrix} \quad (3.23)$$

and similarly the - branch is

$$\psi_s^-(k_x) = \frac{1}{\sqrt{L_x A_s}} e^{ik_x x} \begin{pmatrix} \phi_{s-1}(y - y_c) \\ -iD_s \phi_s(y - y_c) \end{pmatrix} \quad (3.24)$$

where A_s is the normalization constant which is $A_s = 1 + D_s^2$ and D_s is

$$D_s = \frac{(\alpha/l_c)\sqrt{2s}}{E_0 + \sqrt{E_0^2 + 2s\alpha^2/l_c^2}}$$

Now the density of state can be defined as $D(E) = \sum_{sk_x\sigma} \delta[E - E_s^\sigma]$. Considering Gaussian broadening of the width Γ , we get

$$D(E) = \frac{S_0}{(2\pi)^{3/2}} \sum_{s\sigma} \frac{e^{-(E-E_s^\sigma)^2/2\Gamma^2}}{l_c^2 \Gamma} \quad (3.25)$$

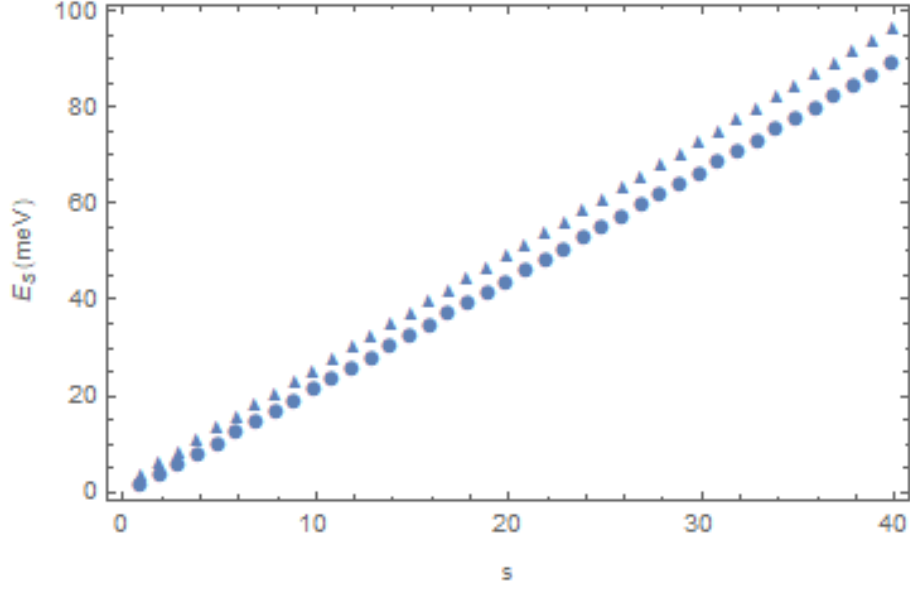


Figure 3.1: Subband Energy E_s versus index s . The circles for $-$ branch and triangles for $+$ branch.

We plotted level energies E_s^- and E_s^+ as a function level index s . In our case here, we have

$$E_1^- \simeq E_0^+$$

It is because of the larger level spacing of $+$ branch as compared to the $-$ branch. It is clear from the graph that increase in level energy of $+$ branch is faster than that of $-$ branch and its slope is also larger than the slope of line of $-$ branch. From the graph it is also noted that

$$E_7^- \simeq \frac{E_5^+ + E_6^+}{2}$$

$$E_{25}^- \simeq \frac{E_{22}^+ + E_{23}^+}{2}$$

DOS modulations are resulted due to the level spacing difference.

3.0.3 Density of States

DOS of 2DEG is calculated with of weak magnetic field, including RSOI term, by using imaginary part self energy. DOS interms of self energy can be defined as

$$D(E) = \text{Im}\left[\frac{\Sigma^-(E)}{(\pi^2 l_0^2 \Gamma_0^2)}\right] \quad (3.26)$$

Here,

Γ_0 =induced impurity level broadening

Where the self energy is

$$\Sigma^-(E) = \sum_s \frac{\Gamma_0^2}{E - \Sigma^-(E) - E_s}$$

Considering lower branch, residue theorem was used to solve summation and ignoring the term $(E_\alpha/\hbar\omega_0)$, we get

$$\Sigma^-(E) = [\pi\Gamma_0^2/\hbar\omega_0] \times \cot(\pi r_+)$$

where $r_+ \simeq \frac{1}{\hbar\omega_0} \left\{ E + E_\alpha/2 - \Sigma^-(E) + \sqrt{E_0^2 + E_\alpha E} \right\}$. According to defination of self energy

$$\Sigma^-(E) = \Delta + i\Gamma/2$$

Comparing both equations and substituting $v = \frac{2\pi}{(\hbar\omega_0)} \left\{ E + E_\alpha/2 - \Delta + \sqrt{E_0^2 + E_\alpha E} \right\}$ and $u = \pi\Gamma/(h\omega_0)$, we get

$$\begin{aligned} \Delta + i\Gamma/2 &= \frac{\pi\Gamma_0^2}{\hbar\omega_0} \cot\left[\frac{(v - iu)}{2}\right] \\ &= \left(\frac{\pi\Gamma_0^2}{\hbar\omega_0}\right) \frac{\sin(v)}{\cosh(u) - \cos(v)} + i \left(\frac{\pi\Gamma_0^2}{\hbar\omega_0}\right) \frac{\sinh(u)}{\cosh(u) - \cos(v)} \end{aligned}$$

In above equation, $\frac{\Gamma}{2} = \left(\frac{\pi\Gamma_0^2}{\hbar\omega_0}\right) \frac{\sinh(u)}{\cosh(u)-\cos(v)}$ is the imaginary part. We can simplify it by using the standard result as

$$\frac{\sinh(u)}{\cosh(u) - \cos(v)} = 1 + 2 \sum_{k=1}^{\infty} e^{-ku} \cos(kv)$$

By applying limit $\hbar\omega_0 \ll \pi\Gamma$, we get $\Gamma/2 = \pi\Gamma_0^2/(\hbar\omega_0)$ for first iteration. As all other terms are smaller than the first term so we only consider $k = 1$ and imaginary part will become $\frac{\Gamma}{2} = \left(\frac{\pi\Gamma_0^2}{\hbar\omega_0}\right) [1 + 2e^{-\pi\Gamma/(\hbar\omega_0)} \cos(u)]$. Now writing this expression in its earlier form

$$\begin{aligned} \frac{\Gamma}{2} = & \left(\frac{\pi\Gamma_0^2}{\hbar\omega_0}\right) \left[1 + 2 \exp \left\{ -2 \left(\frac{\pi\Gamma_0}{\hbar\omega_0}\right)^2 \right\} \right. \\ & \left. \times \cos \left\{ \frac{2\pi}{\hbar\omega_0} \left(E + E_\alpha/2 + \sqrt{E_\alpha E + E_0^2} \right) \right\} \right] \end{aligned}$$

In the similar manner, we can get the same expression with the minor change of sign for upper branch. Finally, we can write the expression for density of states for both branches as

$$\begin{aligned} D^\pm(E) = & \frac{m^*}{2\pi\hbar^2} \left[1 + 2 \exp \left\{ -2 \left(\frac{\pi\Gamma_0}{\hbar\omega}\right)^2 \right\} \right. \\ & \left. \times \cos \left\{ \frac{2\pi}{\hbar\omega} \left(E + \frac{E_\alpha}{2} \mp \sqrt{E_\alpha E + E_0^2} \right) \right\} \right] \end{aligned} \quad (3.27)$$

Without the Rashba and the Zeeman expressions, Eq. (3.27) minimizes to the notable result of [46, 47]:

$$D(E) = \frac{m^*}{\pi\hbar^2} \left[1 - 2 \exp \left\{ -2 \left(\frac{\pi\Gamma_0}{\hbar\omega}\right)^2 \right\} \cos \left(\frac{2\pi E}{\hbar\omega} \right) \right] \quad (3.28)$$

Chapter 4

Results and Discussion

4.1 Analytic Results

To begin with, there are two dispersing methods which are diffusive and collisional scattering that adds into the traveling properties. Starting with diffusive dissipating, which is assumed to limit float speed picked up by the electrons. For our situation, finite group velocity is absent along y-heading because of the k_y decadence in power range. Consequently, the diffusive dissipating to reach the maximum conductivity limit is 0. Whereas, collisional scattering emerges due to cyclotron orbit relocation as charge impurities exist in the system. Moreover, diagonal conductance σ_{xx} is equal to σ_{xx}^{col} because $\sigma_{xx}^{\text{dif}} = \sigma_{yy}^{\text{dif}} = 0$. Also, the magneto resistivity is $\rho_{yy} = \sigma_{xx}/S$ as $S = \sigma_{xx}\sigma_{yy} - \sigma_{xy}\sigma_{yx} = \sigma_{xy}^2$ when σ_{xy} is approximately equal to $n_e e/B$.

An assumption is made that electrons are dissipated elastically by charged impurities in a uniform manner at low temperatures. The basic equation for collisional

conductivity is [48]:

$$\sigma_{\mu\mu}^{col} = \frac{\beta e^2}{S_0} \sum_{\xi, \xi'} f_{\xi} (1 - f_{\xi}) \times W_{\xi, \xi'} \times (\alpha_{\mu}^{\xi} - \alpha_{\mu}^{\xi'})^2 \quad (4.1)$$

In the equation, $W_{\xi, \xi'}$ is equal to transition rate between $|\xi'\rangle$ and $|\xi\rangle$. states. μ from locating operator will have this value $\alpha_{\mu}^{\xi} = \langle \xi | r_{\mu} | \xi \rangle$ when the electron has reached the $|\xi\rangle$ state. Resulting in scattering speed as :

$$W_{\xi, \xi'} = \sum_{\mathbf{q}_0} |U(\mathbf{q}_0)|^2 \times |\langle \xi | e^{i\mathbf{q}_0 \cdot (\mathbf{r} - \mathbf{R})} | \xi' \rangle|^2 \times \delta(E_{\xi} - E_{\xi'})$$

$\mathbf{q} = q_x \hat{x} + q_y \hat{y}$ is the 2D wave vector. Screened impurity potential will be $U(\mathbf{q})$ when resulted from a Fourier transform of

$$U(\mathbf{r}) = (e^2/4\pi\epsilon) (e^{-k_s r}/r)$$

k_s will be the 1/screening length and ϵ is just di-electric constant. Each material will have a different ϵ .

$$U(\mathbf{q}) = 2\pi e^2 / (\epsilon \sqrt{q_x^2 + q_y^2 + k_s^2})$$

Incase $|\mathbf{q}|$ is very small and is $\ll k_s$, then $U(\mathbf{q})$ is approximately equal to $2\pi e^2 / (\epsilon k_s) = U_0$. Then \mathbf{R} and \mathbf{r} will be impurity and the positioning vectors of the electron respectively. All summing up to result in the conductivity of spin up and down electrons [24]

$$\sigma_{xx}^{\pm} = \frac{e^2}{h} \frac{\beta N_I U_0^2}{2\pi \Gamma_0 l_0^2} \sum_s I_s^{\pm} f_s^{\pm} (1 - f_s^{\pm}) \quad (4.2)$$

f_s^{\pm} is known as Fermi-Dirac particles distribution and N_I will be the 2D impurity

density number. Finalizing I_s^\pm as:

$$I_s^\pm = [(2s \pm 1)\mathcal{D}_s^4 - 2s\mathcal{D}_s^2 + 2s \pm 1] / \mathcal{A}_s^2$$

Using the DOS given we can infer terms systematically for the conductivity of spin up and down electrons in Eq. (3.27). The \sum over 's' (quantum No) in Eq. (4.2) could be supplanted as

$$\sum_s \rightarrow 2\pi l_0^2 \int_0^\infty D(E)dE.$$

After a long estimation; we get the logical equations for conductivity of both electron:

$$\frac{\sigma_{xx}^\pm}{\sigma'} = \frac{\tilde{E}_F}{8(\omega\tau)^2} \left[1 + 2 \exp \left\{ -2 \left(\frac{\pi\Gamma_0}{\hbar\omega} \right)^2 \right\} \right. \\ \left. \times A \left(\frac{T}{T_c} \right) \times \cos \left(\frac{2\pi f^\pm}{B} \right) \right] \quad (4.3)$$

where

$$\sigma' = \frac{n_e e^2 \tau}{m^*} = \text{Drude conductivity,}$$

$$\tilde{E}_F = \left[1 + \frac{1}{2} \frac{E_\alpha}{q E_F} \mp \frac{3}{2} \sqrt{\frac{E_\alpha}{E_F}} \right]$$

$$A \left(\frac{T}{T_c} \right) = \left(\frac{T}{T_c} \right) \times \frac{1}{\sinh \left(\frac{T}{T_c} \right)}$$

with $T_c = \hbar\omega/2\pi^2 k_B$. Using diverse frequencies, Spin up and down will oscillate their conductivities as given:

$$f^\pm = \frac{m^*}{\hbar e} \left[E_F + \frac{E_\alpha}{2} \mp \sqrt{E_0^2 + E_\alpha E_F} \right] \quad (4.4)$$

Now the conductivity can be written as

$$\frac{\sigma_{xx}}{\sigma_0} \simeq \frac{1}{4(\omega\tau)^2} \left[1 + 2 \exp \left\{ -2 \left(\frac{\pi\Gamma_0}{\hbar\omega} \right)^2 \right\} A \left(\frac{T}{T_c} \right) \right. \\ \left. \times \cos \left(2\pi \frac{f_a}{B} \right) \cos \left(2\pi \frac{f_d}{B} \right) \right] \quad (4.5)$$

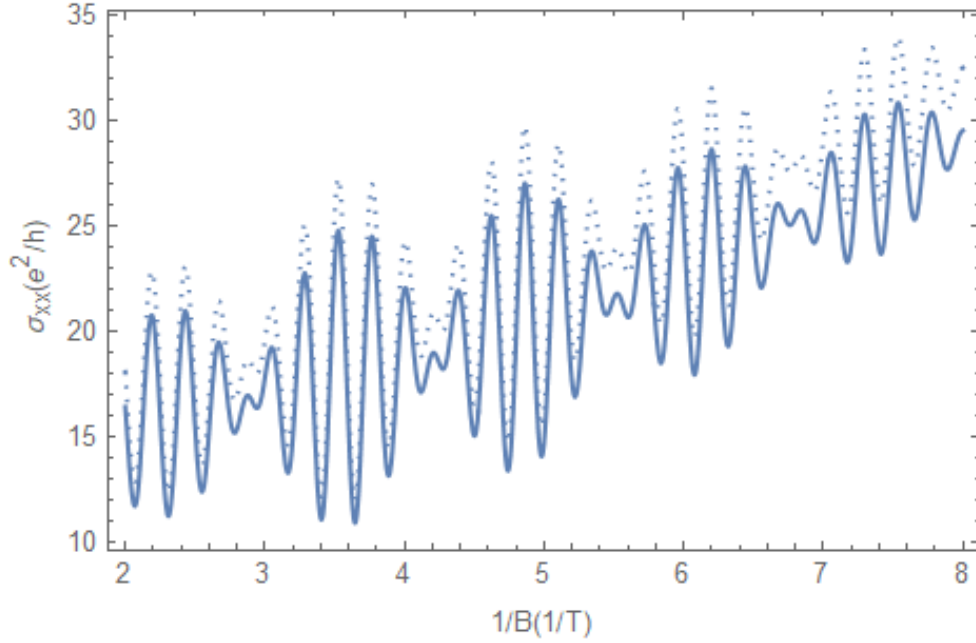


Figure 4.1: Plots of the analytical (solid) and exact (dashed) expressions of the total conductivities vs $1/B$.

When $f_d = [f^+ - f^-]/2$. and $f_a = [f^+ + f^-]/2$. It unmistakably represents that entire conductivity generates different beating outlines when in adequacy of SdH motions. From Fig. 4.1 we can see scientific consequence of the entire complete conductivity along with precise numbered outcomes using Eq. (4.2). Diagnostic equation gives a beating outline pattern which is in amazing concurrence with the precise numbered outcomes, especially in area where a node is present. Fig. 4.1

Variables: $\alpha = 10^{-11}eV - m, \Gamma_0 = 0.02meV$, $e-$ density $n_e = 3 \times 10^{15}/m^2$ and $e-$, $(m^*) = 0.05m_0$ along with m_0 being the free $e-$ mass, and temperature at $1K$. Oscillations in between two progressive or successive nodes are:

$$N_{osc} = f_a \Delta \left(\frac{1}{B} \right) = \frac{m^*}{\hbar e} \left(E_F + \frac{E_\alpha}{2} \right) \left(\frac{1}{B_{j+1}} - \frac{1}{B_j} \right)$$

Each Jth J node will have its own corresponding magnetic field $(B_j) \cos(2\pi f_d/B)$, the last cosine value's $f_d = \frac{m^*}{Le} \sqrt{E_0^2 + E_\alpha E_F}$, (frequency difference) depends on the magnetic force field itself, which makes it non-periodic in B inverse.

When observed, it is known that due to magnetic field depending on f_d , the beating pattern in turn will have non periodic manners. At B_j node the cosine terms will have the following conditions $B = B_j = 0$ which will give us the following:

$$\sqrt{4E_0^2 + \Delta_s^2} = \hbar\omega_j \left(j + \frac{1}{2} \right) \quad (4.6)$$

Where j are the beating nodes i.e. $1, 2, 3, \dots, \Delta_s = 2k_F\alpha$ is zero field spin spitting energy and $\omega_j = eB_j/m^*$ which will allow us to calculate magnetic field for any beat node.

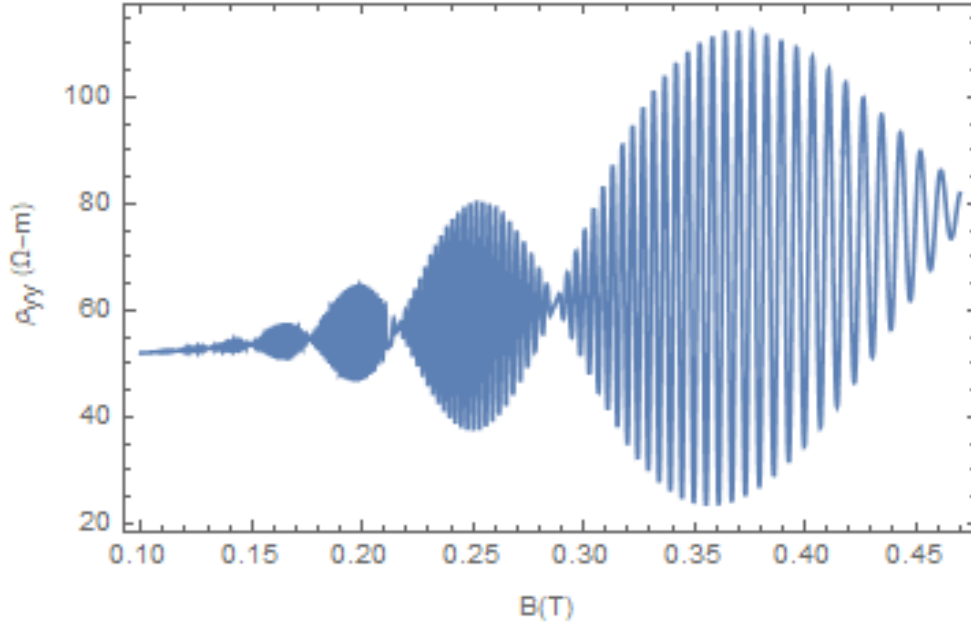


Figure 4.2: Plot of resistivity vs magnetic field B.

$$B_j = \frac{2m^*}{e\hbar} \frac{\Delta_s}{\sqrt{(2j+1)^2 - (g-2)^2}}$$

The equation above is obtained using self consistency Born approximation mentioned in Ref.[49].

4.2 Side by side assessment with known experiment

Our diagnostic articulations are tested by ascertaining the places of nodes, the *ZFSS* energy, and the beating patterns between two successive/progressive nodes and afterward contrasting them with the known experimental perceptions. Now, if we recreate those experimental beating motion values, we will have to take resistiv-

ity as a component of the magnetic Field in Fig.4.2. In Fig.4.2, the experiment will have the following variables for sample A: $\alpha = 3.76 \times 10^{-12}eV - m, \Gamma_0 = 1.5meV$, $e-$ density $n_e = 1.75 \times 10^{16}m_2$, $e-$ effective mass $m^* = 0.046m_0$ with m_0 a as the free $e-$ and temperature at $1.5K$.

node	Beat points (B) in Tesla	$\Delta_s^A(10^{-3})$ eV	$\alpha(10^{-12})eVm$
1	0.874	2.45	3.70
2	0.461	2.64	3.99
3	0.292	2.44	3.69
4	0.228	2.50	3.77
5	0.184	2.48	3.75
6	0.154	2.46	3.72

Table 4.1: Sample A:ZFSS and Rashba interaction SOI power at different node locations

Its reassuring to see oscillations between any 2 nodes and the position of beat nodes are coordinating almost perfectly when compared with the experimental values. We might want to decide the ZFSS energy and consequently the Rashba's interaction SOI power by utilizing the places of beat nodes for 3 separate tests A, B, and C utilized in Ref.[19]. The variables utilized are: $m^* = 0.046m_0$ and $n_e = 1.75 \times 10^{16}/m^2, 1.65 \times 10^{16}m^2, 1.46 \times 10^{16}m^2$ for each A, B, and C test, correspondingly [19]. Utilizing Eq. (4.8), for the starting 6 nodes we decide ZFSS energy and the SOI mentioned in the table above. ZFSS energy's average value at the Fermi level is $\Delta_s^A = 2.50meV$ and the RSOI value is $3.77 \times 10^{-12}eV - m$. Our outcomes are almost equivalent to got in Ref.[19]. Additionally, for sample test B, the acquired outcomes are given in the Table below:

ZFSS energy's average value in this is $\Delta_s^B = 2.7meV$ and the RSOI strength α is equal to $4.20 \times 10^{-12}eV - m$. Moving on to sample test C, the average value acquired is $\Delta_s^C = 1.76meV$ and the RSOI strength α is $4.19 \times 10^{-12}eV - m$. These outcomes

node	Beat points (B) in Tesla	$\Delta_s^B(10^{-3})$ eV	$\alpha(10^{-12})eVm$
1	0.295	2.70	4.20
2	0.201	2.70	4.20
3	0.153	2.68	4.16
4	0.129	2.78	4.32
5	0.104	2.68	4.16

Table 4.2: Sample B: ZFSS and Rashba α SOI power at different node locations

are incredibly concurrent to the outcome achieved in Ref.[19]. Presently another examination is recommended where the SOI strength has been noted down [18]. By remembering the places of the 2 progressive nodes, we could likewise compute the SOI strength. Utilizing the variables in Ref.[18], we achieve the RSOI strength α as $0.9 \times 10^{-9}eV - cm$ which is the exact same of Ref.[18]. Also, the oscillations between 2 beating nodes in Ref[19] ($j = 1$ and $j = 2$) is 36 [show in figure of Ref.[19]. Utilizing the variables from test [19], we acquire $N_{osc} = 37$. This value precisely coordinates with the experimented values. Moreover, another examination is considered changing SOI strength by differing the gateway voltages. Door voltages were set as $V_g = 0.3$ and $1.5V$, through which the determined oscillations between 2 nodes had N_{osc} values of 27 and 30, separately. These numbers are equivalent to the immediate observations.

Chapter 5

Conclusion

In conclusion, the beating patterns from 2DEG in the SdH oscillations were conceptualized. We experimented and inferred the DOS in a 2DEG for spin-down and spin-up electrons with the RSOI in the nearness of a magnetic force field. The DOS diagnostic articulations will be valuable to ascertain different properties, systematically. We have given diagnostic calculations of the magneto conductivities for spin-down and spin-up electrons, that'll waver with 2 intently different frequencies. The conductivity varies with frequencies that rely on e^- density, strength of SOI, and furthermore the outside magnetic force field. The regular way to get the basic condition has been used. It decides the ZFSS power by remembering the force field's relation to any beat nodes. The total oscillations in between any 2 beating nodes can be effectively calculated from our equation. Most of those oscillations in a beat precisely coordinate with the experimented values. The non-uniform beating design relies on the frequency difference between spin-up and down electrons present in the same magnetic force field.

Bibliography

- [1] Žutić, Igor, Jaroslav Fabian, and S. Das Sarma. "Spintronics: Fundamentals and applications." *Reviews of modern physics* 76.2 (2004): 323.
- [2] Fabian, Jaroslav, et al. "Semiconductor spintronics." *arXiv preprint arXiv:0711.1461* (2007).
- [3] Cahay, Marc, and Supriyo Bandyopadhyay. "Introduction to Spintronics." (2008).
- [4] Datta, Supriyo, and Biswajit Das. "Electronic analog of the electro-optic modulator." *Applied Physics Letters* 56.7 (1990): 665-667.
- [5] Bandyopadhyay, S., and M. Cahay. "Alternate spintronic analog of the electro-optic modulator." *Applied physics letters* 85.10 (2004): 1814-1816.
- [6] Tutuc, Emanuel, et al. "In-plane magnetic field-induced spin polarization and transition to insulating behavior in two-dimensional hole systems." *Physical review letters* 86.13 (2001): 2858.
- [7] Lu, Jian Ping, et al. "Tunable spin-splitting and spin-resolved ballistic transport in GaAs/AlGaAs two-dimensional holes." *Physical review letters* 81.6 (1998): 1282.

- [8] Ganichev, S. D., et al. "Spin-galvanic effect." *Nature* 417.6885 (2002): 153-156.
- [9] Dyakonov, Mikhail I., and V. I. Perel. "Current-induced spin orientation of electrons in semiconductors." *Physics Letters A* 35.6 (1971): 459-460.
- [10] Murakami, Shuichi, Naoto Nagaosa, and Shou-Cheng Zhang. "Dissipationless quantum spin current at room temperature." *Science* 301.5638 (2003): 1348-1351.
- [11] Dresselhaus, Gene. "Spin-orbit coupling effects in zinc blende structures." *Physical Review* 100.2 (1955): 580.
- [12] Wang, X. F., and P. Vasilopoulos. "Magnetotransport in a two-dimensional electron gas in the presence of spin-orbit interaction." *Physical Review B* 67.8 (2003): 085313.
- [13] Lommer, G., F. Malcher, and U. Rossler. "Spin splitting in semiconductor heterostructures for $B \rightarrow 0$." *Physical review letters* 60.8 (1988): 728.
- [14] e Silva, EA de Andrada, G. C. La Rocca, and F. Bassani. "Spin-split subbands and magneto-oscillations in III-V asymmetric heterostructures." *Physical Review B* 50.12 (1994): 8523.
- [15] Stormer, H. L., et al. "Energy structure and quantized Hall effect of two-dimensional holes." *Physical review letters* 51.2 (1983): 126.
- [16] Stein, D., K. V. Klitzing, and G. Weimann. "Electron Spin Resonance on $GaAs - Al_xGa_{1-x}As$ Heterostructures." *Physical review letters* 51.2 (1983): 130.

- [17] Bychkov, Yu A., and Emmanuel I. Rashba. "Oscillatory effects and the magnetic susceptibility of carriers in inversion layers." *Journal of physics C: Solid state physics* 17.33 (1984): 6039.
- [18] Luo, J., et al. "Effects of inversion asymmetry on electron energy band structures in GaSb/InAs/GaSb quantum wells." *Physical Review B* 41.11 (1990): 7685.
- [19] Das, B., et al. "Evidence for spin splitting in $In_xGa_{1-x}As/In_{0.52}Al_{0.48}As$ heterostructures as $B \rightarrow 0$." *Physical Review B* 39.2 (1989): 1411.
- [20] Nitta, Junsaku, et al. "Gate Control of Spin-Orbit Interaction in an Inverted In 0.53 Ga 0.47 As/In 0.52 Al 0.48 As Heterostructure." *Physical Review Letters* 78.7 (1997): 1335.
- [21] Engels, G., et al. "Experimental and theoretical approach to spin splitting in modulation-doped $In_xGa_{1-x}As/InP$ quantum wells for $B \rightarrow 0$." *Physical Review B* 55.4 (1997): R1958.
- [22] Heida, J. P., et al. "Spin-orbit interaction in a two-dimensional electron gas in a InAs/AlSb quantum well with gate-controlled electron density." *Physical Review B* 57.19 (1998): 11911.
- [23] Das, B., S. Datta, and R. Reifenberger. "Zero-field spin splitting in a two-dimensional electron gas." *Physical Review B* 41.12 (1990): 8278.
- [24] Wang, X. F., and P. Vasilopoulos. "Magnetotransport in a two-dimensional electron gas in the presence of spin-orbit interaction." *Physical Review B* 67.8 (2003): 085313.

- [25] Ingenhoven, Philip Christopher. Spin-dependent electronic and transport properties of unconventional conductors: a thesis presented in partial fulfilment of the requirements for the degree of Doctor of Philosophy in Physics at Massey University, Palmerston North, New Zealand. Diss. Massey University, 2010.
- [26] Bhushan, Bharat. "Introduction to nanotechnology." Springer handbook of nanotechnology. Springer, Berlin, Heidelberg, 2017. 1-19.
- [27] Ihn, Thomas. Semiconductor Nanostructures: Quantum states and electronic transport. Oxford University Press, 2010.
- [28] Porgilsson, Gunnar. Modeling transport through semiconductor nanostructures with Rashba spin-orbit interaction. Diss.
- [29] Grosso, G., and G. P. Parravicini. "Solid State Physics, Chapter 11." (2000): 389-414.
- [30] Nobel, Prize. "Nobel Prize in Physics-2005." (2005).
- [31] Datta, Supriyo, and Biswajit Das. "Electronic analog of the electro-optic modulator." Applied Physics Letters 56.7 (1990): 665-667.
- [32] Dietl, Tomasz. "Origin and control of ferromagnetism in dilute magnetic semiconductors and oxides." Journal of Applied Physics 103.7 (2008): 07D111.
- [33] Wu, M. W., J. H. Jiang, and M. Q. Weng. "Spin dynamics in semiconductors." Physics Reports 493.2-4 (2010): 61-236.
- [34] Griffiths, David J., and Darrell F. Schroeter. Introduction to quantum mechanics. Cambridge University Press, 2018.

- [35] Greiner, Walter. Relativistic quantum mechanics. Vol. 2. Springer, Berlin, 2000.
- [36] Winkler, R., et al. Spin-Orbit Coupling in Two-Dimensional Electron and Hole Systems. Vol. 41. Springer, 2003.
- [37] Dyakonov, M. I., and V. I. Perel. "Spin relaxation of conduction electrons in noncentrosymmetric semiconductors." Soviet Physics Solid State, Ussr 13.12 (1972): 3023-3026.
- [38] "J. Singleton, Band Theory and Electronic Properties of Solids, Oxford University Press, 2001, xvi+ 222p., 25× 19cm, 10, 540,(Oxford Master Series in Condensed Matter Physics), 57.9 (2002): 683-684.
- [39] Onsager, Lars. "Reciprocal relations in irreversible processes. I." Physical review 37.4 (1931): 405.
- [40] Tregurtha, David. The transport properties of electrons and holes in a silicon quantum well. Diss. University of Bath, 2014.
- [41] Hall, Edwin H. "On a new action of the magnet on electric currents." American Journal of Mathematics 2.3 (1879): 287-292.
- [42] Ando, Tsuneya, Yukio Matsumoto, and Yasutada Uemura. "Theory of Hall effect in a two-dimensional electron system." Journal of the Physical Society of Japan 39.2 (1975): 279-288.
- [43] Klitzing, K. V., Gerhard Dorda, and Michael Pepper. "New method for high-accuracy determination of the fine-structure constant based on quantized Hall resistance." Physical Review Letters 45.6 (1980): 494.
- [44] Phillips, P. "Advanced Solid State Physics Westview." Cambridge MA (2003).

- [45] Bassani, Franco. Encyclopedia of condensed matter physics. Elsevier acad. press, 2005.
- [46] Ando, Tsuneya, and Yoshimasa Murayama. "Landau-level broadening in GaAs/AlGaAs heterojunctions." Journal of the Physical Society of Japan 54.4 (1985): 1519-1527.
- [47] Zhang, Chao, and Rolf R. Gerhardts. "Theory of magnetotransport in two-dimensional electron systems with unidirectional periodic modulation." Physical Review B 41.18 (1990): 12850.
- [48] Vasilopoulos, Pagiotis, and Carolyn M. Van Vliet. "Linear response theory revisited. IV. Applications." Journal of mathematical physics 25.5 (1984): 1391-1403.
- [49] Novokshonov, S. G., and A. G. Groshev. "Diffusive magnetotransport in a two-dimensional electron gas in the presence of Rashba spin-orbit interaction." Physical Review B 74.24 (2006): 245333.